

The term climate modeling, as used here, includes (1) forecasts of climate with global AOGCMs that simulate the physical system's response to radiative-forcing scenarios that assume a specific trajectory for anthropogenic and natural gas and aerosol emissions, (2) initial-value simulations on seasonal to annual time scales, (3) the production of model-based analyses of the present climate, and (4) model experiments that evaluate the response of the climate system to anthropogenic changes in the landscape, say associated with continued urbanization or the expansion of agriculture. Thus, the term climate modeling refers to the use of a model to define the state of Earth's physical system on time scales of seasons to centuries. As we will see, the specifics of the modeling process depend on the time scale. Typically not included are monthly forecasts (e.g., Vitart 2004), which bridge the gap between medium-range forecasting and seasonal forecasting. If the AOGCM forecasts or the global-reanalysis data sets are used as input to a regional (mesoscale) model or a statistical procedure for correlating the large- and small-scale climate of a region, the process is called climate downscaling.

The material about the modeling of weather that has been presented so far in this book also has direct application to the problem of climate modeling. The climate is, after all, just the aggregate behavior of many thousands of individual weather events. So, errors in the model's numerical algorithms, shortcomings in physical-process parameterizations, and incorrectly represented land–ocean–atmosphere interactions may affect climate predictions just as severely as weather predictions. In fact, some model errors that are acceptable for forecasts of a day to a couple of weeks may severely impact model integrations that extend over decades and centuries. Included would be slow rates of mass gain or loss, or errors in the representation of radiation such that there are nonphysical drifts in the temperature. Alternatively, there are serious errors that can develop in weather predictions, such as phase errors in waves, that may have less consequence for climate prediction.

This chapter will begin with a review of global climate modeling, including how the models differ from those used in weather prediction, how their skill is verified using simulations of current or past climates, the differences in approach between seasonal and longer radiatively forced predictions, a summary of the models being employed, and the use of ensemble methods. The section after that summarizes how global models are used to create reanalyses of the current climate. This is followed by a section on climate downscaling, where downscaling is motivated by the often-stated fact that “all climate is local”. That is, the human response to climate change takes place at the local level, and depends on local economic, agricultural, and societal factors. Thus, this need for fine-scale information requires the use of LAMs or statistical methods that employ input from AOGCM

forecasts or global reanalyses. The final section describes the use of models to estimate the effects on climate of anthropogenic landscape changes.

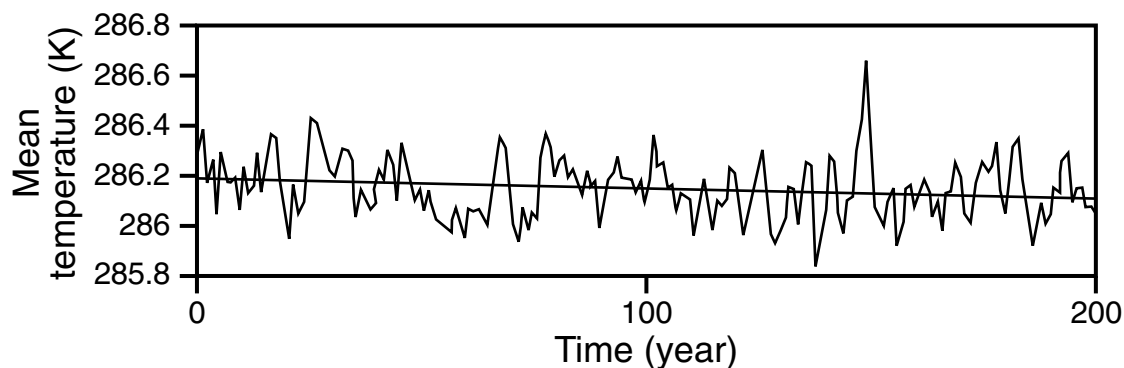
## 16.1 Global climate prediction

Numerical methods and physical-process parameterizations used for modeling the global atmosphere, with applications to both weather and climate prediction, were described in earlier chapters. However, global climate models must also represent many additional physical processes in the hydrosphere (including ocean circulations), the cryosphere (land and sea ice), the lithosphere (land surface), and the biosphere, and how they interact with each other. For most weather forecasts of up to two weeks, the sea-surface temperature; the health, spatial extent, and types of vegetation; the extent of the permafrost, glaciers, and sea ice; the chemical composition of the atmosphere; etc., can be specified and assumed to be invariant during the model integration. However, this is not the case with climate simulations with durations of years to decades to centuries. To the greatest extent possible, the physical subsystems need to fully interact in the coupled model because they are part of the complex of, sometimes nonlinearly interacting, processes that affect climate. This is why such models are sometimes referred to as climate-system models rather than simply climate models.

### 16.1.1 Experimental designs for global climate-change studies

Before models are employed for forecasting future climates, their ability to reasonably replicate the current or past climates must be confirmed. Naturally, this success is not a guarantee of an accurate climate forecast because some model representations of physical processes are tuned for the current climate, and may not be as accurate in a different climate regime. Nevertheless, for future-climate studies using AOGCMs, and LAMs or statistical methods to downscale from AOGCM simulations, the responsible experimental approach is to first apply the modeling system for present or past climates to quantify the model's performance. This verification process will be described in Section 16.1.3.

The annual-mean weather varies from year to year and decade to decade, partly because of internal variability in the climate system resulting from natural long-time-scale physical processes (related to deep-ocean circulations, the land surface, and ice). For example, the heavy black line in Fig. 16.3, later in the chapter, shows the evolution of the global-average observed surface temperature during the twentieth century. Superimposed on the long-term upward trend in temperature are many scales of variation, from a few years to multiple decades. Research has shown that the long-term trend is probably of anthropogenic origin, while the decadal and shorter oscillations represent internal variability. If the goal is to quantify the effects of anthropogenic forcing – e.g., the Intergovernmental Panel on Climate Change (IPCC) effort – simulated changes associated with internal variability should be filtered in some way in order to avoid misinterpreting natural variability as anthropogenic effects. This is especially important when downscaling from AOGCM simulations, where

**Fig. 16.1**

Time series of the annual-mean surface air temperature from a control simulation of the US Geophysical Fluid Dynamics Laboratory AOGCM. From AchutaRao *et al.* (2004).

only short segments of time (referred to as slices) are simulated for the present and future climates. That is, the simulated difference between the current and future downscaled climate will depend on the phase of the internal variations at the times of the slices.

There are a few approaches for modeling climate change, where the method of choice depends on the objective. For estimation of the effects on climate of radiative forcing from optically active gases and aerosols of anthropogenic origin, it is typical to first generate a present-climate AOGCM control, or reference, simulation for a period of centuries, using a constant, present radiative forcing. These simulations sometimes require thousands of years of spin up in order to allow the deep ocean circulations sufficient time to develop. Figure 16.1 illustrates the global-mean surface air temperature from such a control simulation, where the multi-year (internal) variability in this current-climate regime results from slow ocean–atmosphere interactions. Then, a future-climate projection is made, starting at an arbitrary time in the control simulation, using a particular future-emissions scenario for aerosols and optically active gases. See Nakicenovic (2000) for a description of the different scenarios used in the IPCC modeling experiments. Because longer-term trends associated with the climate change will be superimposed on the internal variations, the simulated change in a variable will depend on the phase and amplitude of the internal anomalies at the start time of the simulation. Choosing a different start time will result in a different pattern to the internal variability. Thus, running an ensemble of simulations with different start times, and averaging, will remove some of the effects of the internal variation. The same model can be used for each simulation in the ensemble, but a similar filtering can be achieved by using a variety of different models, such as the suite used in the IPCC simulations (IPCC 2007). As evidence of this smoothing, note that the individual simulations (light gray lines) depicted later in Fig. 16.3 have much greater temporal variance than does the ensemble-average (dark gray line).

Coupled AOGCMs can also be used to forecast the change in climate – both internal and anthropogenic – on time scales of seasons to years. For example, the drought in the Sahel during the last few decades of the twentieth century was likely, at least partially, caused by natural internal variability in the climate system. Thus, forecasts must accurately define the prevailing phases and amplitudes of many internal processes such as ENSO, the Pacific

decadal oscillation, the North Atlantic oscillation, and changes in the meridional overturning circulation in the Atlantic Ocean basin. To represent the internal oscillations, initial conditions must be employed that define the state of the entire physical system. Accurately defining the state of the deep-ocean waters is clearly a great challenge. Section 16.1.4 summarizes the process by which these initial-value climate predictions are produced.

As with weather prediction, multi-model ensembles can be used to improve the predictability of climate. In particular, the unpredictable aspects in the model solution can cancel when aggregating the simulations, so that the ensemble mean is superior to the individual members. However, unlike ensemble weather prediction, where the members can be chosen so that they have roughly equal skill, that is not possible when members are based on disparate models from various organizations worldwide. The use of such multi-model ensembles is central to the IPCC assessments of climate change (IPCC 2007). Ensemble methods used in climate simulation are discussed in Section 16.1.6.

Another category of experiments has been used to define the strength of the internal feedback processes that amplify or dampen the system's response to the radiative forcing. Metrics for this sensitivity include a quantity called the *equilibrium climate sensitivity*, which is defined as the equilibrium surface temperature change that results from a doubling of the carbon dioxide concentration in a model atmosphere, and it is expressed in degrees Celsius. An alternative measure of the strength of the feedbacks is the *transient climate response*, which is the surface air temperature change that results from a carbon dioxide concentration increase of  $1\% \text{ yr}^{-1}$ , until the doubling point is reached. After reaching this point, the system is given sufficient time to come to equilibrium. Differences among models in terms of their future-climate predictions are partially a result of the feedback strengths measured here. See Box 10.2 in Meehl *et al.* (2007) and Section 8.6 in Randall *et al.* (2007) for further discussions of the concept of climate sensitivity.

For estimation of the effects on global (and regional) climate of future anthropogenic landscape changes, models can be run for long periods of time with and without the change. Such studies are important because of the potential climate impacts of future large-scale deforestation, conversion of grassland to agricultural crops, expansion of cities, expansion and contraction of the irrigation of agricultural crops, and diversion of water from lakes causing them to shrink in size or disappear altogether. Depending on the scale of the climate response to be evaluated, a global model can be used for the study, or a LAM can be employed to resolve mesoscale processes.

## 16.1.2 Special model requirements

Climate models differ in a variety of ways from the traditional weather-forecast models described elsewhere in this book. The following sections review some of these differences.

### Land-surface and ice modeling

Surface-process components of weather-prediction models were discussed earlier in Chapter 5. However, there are a number of land-ice processes that operate on longer, climate time scales that must be considered here. Ice (cryospheric) processes, on both land

and sea, are also included in this discussion. The reader should see Sections 8.2.3 and 8.2.4 of Randall *et al.* (2007), and the references in the land and sea-ice columns of Table 16.1 in this chapter, for additional information. The terminology used in this table deserves elaboration. For sea-ice dynamics, the word “leads” refers to the representation in the models of narrow areas of open-water in cracks within the ice. In these areas, the heat and water-vapor fluxes are extremely large. The word “rheology” refers to whether the models represent the slow “flow” of ice sheets. None of the models represents the dynamics of ice-sheet melting (e.g., Greenland and Antarctica), which is why there is great uncertainty about sea-level rise. In the column that pertains to land processes, “canopy” refers to the explicit treatment of vegetation effects, “routing” refers to whether rainwater or snow/ice-melt water are routed into stream channels on the land surface, “layers” refers to the use of a multi-layer soil model, and “bucket” refers to a simple method for treating soil hydrology. Two community-developed land-surface-process models that are commonly used for climate applications are the Community Land Model (Oleson *et al.* 2008) and the Common Land Model (Dai *et al.* 2003).

One of the major important advances in newer-generation climate models is the inclusion of terrestrial-biosphere models that treat some terrestrial carbon sources and sinks. The processes that are represented involve both soil carbon cycling and vegetation. For example, dynamic-vegetation models simulate the response of the vegetation to changes in carbon dioxide concentrations and to climate variables (e.g., precipitation, temperature) that affect vegetation health. In addition, there is higher-resolution modeling of the over-land flow of water, the inclusion of plant root dynamics, the use of multi-layer snowpack models, and the prediction of the motion and thickness of sea ice. However, as with efforts to improve other aspects of climate models, it is unclear how well the new representations of these land-surface and cryospheric processes will perform in greatly different climate regimes.

It is important to be reminded of the need to employ surface-process models that can adequately represent land–biosphere–cryosphere–atmosphere feedbacks. For example, the simulated soil moisture influences dynamic-vegetation models, and the state of the vegetation determines its quantitative influence in the carbon cycle. Pielke *et al.* (1999a) illustrate the importance of land–atmosphere interactions by calculating the time after which the initial soil-moisture conditions became unimportant in seasonal weather prediction with an Atmospheric General Circulation Model (AGCM). They concluded that the model’s memory of the initial soil moisture lasted 200–300 days. A general discussion is provided, along with a good list of references, of the importance of properly modeling the landscape (e.g., landcover type, leaf-area index, soil moisture) changes associated with drought and climate change. There are also plentiful examples provided of the long-distance impacts on climate of anthropogenic landscape changes, which need to be accounted for as well in climate simulations.

### Ocean-circulation modeling

The ocean and atmosphere interact through fluxes of heat, water vapor, and momentum. For weather-prediction purposes, it is generally sufficient to represent the ocean through

specified surface temperature and salinity (which affects saturation vapor pressure) patterns, and the use of a wind-speed dependent roughness length. That is, except as a result of extreme wind speeds, such as in hurricanes, the feedback between the ocean and the atmosphere during the period of a forecast is sufficiently small that most weather-prediction models are not coupled to ocean models. However, on time scales of longer than a few weeks the ocean properties can evolve considerably, and an active ocean-circulation model should be employed. The ocean models run simultaneously with the atmospheric models, out of necessity because of the two-way interaction, but they typically have different horizontal resolutions than do the atmospheric models. See Section 8.2.2 of Randall *et al.* 2007, and the ocean-modeling references in Table 16.1, for additional information about the ocean component of global-climate models.

### Physical-process parameterizations

The challenges of parameterizing physical processes in climate models do not differ greatly from those associated with global weather-prediction models. Exceptions include the fact that small errors in the representation of processes may be acceptable for forecasts of weeks, but over much longer time periods the cumulative error can cause unacceptable drifts in simulated climate. This problem can be addressed to some degree by “tuning” model parameters (in parameterizations) so as to optimize simulation results, such as in the atmosphere–ocean flux corrections described below. But, this process is not intuitively appealing because tuning the model to the current climate does not ensure an equally positive effect for future climates. Furthermore, adjusting a particular parameter does not necessarily give you a better model solution for the right reason. A partial remedy to this problem is to use higher-resolution global models that explicitly resolve processes such as convection. The use of higher-resolution regional models for downscaling may allow better explicit local representation of processes, but that has no benefit for the simulation of the global climate by the parent AOGCM. Lastly, because global climate models typically have coarser horizontal resolution than do global weather-prediction models, parameterizations may be more suitable for one application than the other because their performance is sometimes scale dependent.

### Conservation properties of dynamical cores

The general issues associated with the conservation of properties such as mass and energy by models were discussed in Chapter 3. This need for conservation is clearly more critical for long climate-time-scale simulations than for weather-prediction time scales of days to weeks. That is, small rates of error accumulation may not be damaging for short model integrations, but may be for long ones. For example, Boville (2000) states that, for climate models, energy must be conserved to tenths of a watt per square meter. Williamson (2007) points out that one of the energy conservation problems that must be addressed is the accumulation of energy in small scales through aliasing, discussed in Section 3.4.5. See Thuburn (2008) for a good general discussion of conservation issues for the dynamical cores of climate and NWP models.

## Initial conditions

For IPCC-scenario climate-change simulations, or those involving projected landscape changes, it is sufficient to initialize the model with any realization of the weather associated with current climate conditions. However, the aforementioned seasonal to decadal forecasts that hope to represent the phase and amplitude of internal climate variations are initial-value problems. Thus, the states of the atmosphere, ocean, biosphere, cryosphere, and lithosphere must be defined by initial values.

For experiments that might involve more drastic perturbations to the climate or external forcing, it is useful to keep in mind the distinction between *transitive* and *intransitive* climate systems (Lorenz 1968). A transitive climate system is one in which there is only one permitted set of long-term climate statistics – that is, given a particular set of external forcing parameters for the atmosphere, such as the orography, the solar input, Earth's rotation rate, etc., there is only one stable long-term climate. In contrast, an intransitive system has more than one possible stable climate, with the prevailing climate determined by the present state of the system. A special type of system is an *almost-intransitive* one, in which the climate remains within a regime for a finite time, with the system then migrating into another equally acceptable regime without any change in the external forcing. In other words, climate regimes have sufficient “inertia”, in a dynamic sense, to be self-perpetuating for a period of time. This is consistent with the observed situation where distinct periods of prolonged regional drought can transition abruptly into periods with normal or abundant precipitation. Thus, for intransitive and almost-intransitive climate systems, the initial conditions that define the present state of the system can determine the resulting climate regime.

## Flux corrections

Small errors in the simulated fluxes of heat, water vapor, and momentum at the air–sea interface can cause climate-model solutions to drift to an unrealistic climate state. To address this problem of some models, artificial corrections have been added to the flux terms in the equations. This practice is of obvious concern because it is nonphysical, and the corrections cannot be targeted for those physical situations where the errors may dominate. In the first two Climate Model Intercomparison Projects, which took place in the 1990s, over half of the models were flux corrected (Reichler and Kim 2008), whereas in the third and latest comparison, less than one-quarter of the models were flux corrected (for example, see the flux-adjustments column in Table 16.1 later in the chapter).

### 16.1.3 Verification of global climate-change models for past or current climates

As noted above, the only way of gaining confidence in the ability of a global climate model to simulate future climate is to evaluate its ability to replicate the conditions of past climates or the current climate. The advantage of using recent climates for this purpose is that meteorological observations are more plentiful. However, the opportunity to fully test the ability of models to simulate climate change is limited because recent climate variation



has been small compared with the potential future changes that must be predicted. Thus, there have also been efforts to test models by running them for paleoclimate periods, during which climates have varied widely. The obvious drawback is that there are large uncertainties in the external forcing as well as in the prevailing climate variables themselves, where various proxies need to be used to estimate the latter. In addition, simulating climate change that takes place over very long, paleoclimate time periods is computationally impractical with traditional full-physics models.

It is arguable that this process should involve verification of the model's ability to simulate individual weather events, as well as the long-term statistics of the events – the climate. That is, both the specific characteristics of the simulated weather events (e.g., tracks, intensity, and frequency of midlatitude storms; characteristics of easterly waves in the tropics; properties of low-level jets near coastlines and mountains) and the climate statistics of the aggregated weather events should be compared with the actual properties of the weather and climate as defined by archived observations. Without evaluating the model's rendering of the events that make up the climate, there is the risk that the statistics could be correct for the wrong reason, leading to errors when applying the model for future climates.

Because climate models are extremely complex, components are often developed and tested individually. For example, the properties of numerical methods can be isolated and evaluated much more effectively without the use of the physical-process parameterizations. And the physical-process parameterizations can be studied through the use of case studies, possibly with special field-program data for verification. Only when a climate model has been tested as thoroughly as possible at the component level, should its performance be evaluated in the context of approximating the entire climate system.

Climate-model verification has employed a number of metrics for comparing the model solution with observations, including global means of variables, composite global indices based on a number of variables, spatial patterns of variables, the temporal variability of regional climates over times scales as large as decades (internal climate-system variability), the ability of the model to replicate specific well-documented features of the current climate (e.g., ENSO), and the ability of the model to simulate regional extremes of variables on various time scales. A good general reference for this subject is Section 8.3 of Randall *et al.* (2007).

### Verification of global-average climate statistics

One of the challenges in climate-model verification is simply deciding upon what variables best represent climate and can serve as metrics of overall errors in its simulation. This choice is not easy because of the many variables associated with the state of the atmosphere, hydrosphere, cryosphere, lithosphere, and biosphere. Some studies simply use global-mean surface air temperature (e.g., Min and Hense 2006). Others use composite error indices that are based on a broad range of climate variables (Murphy *et al.* 2004, Reichler and Kim 2008). Others use a few traditional error statistics, where Boer and Lambert (2001) and Taylor (2001) summarize them in graphical form. Another complication in the model verification process results from the fact that the observations that define the current climate are not an independent measure of the model accuracy because they have



already been used to tune the model physical-process parameterizations. Nevertheless, we have no choice but to use them for the verification. This issue may be somewhat mitigated by the use of higher-resolution climate models that require less parameterization of processes.

An example of a thorough verification of models for current climates is described in Reichler and Kim (2008). In this study, numerous models (see Table 16.1) were compared, using a performance index that was based on many variables, for simulations from three different Climate Model Intercomparison Projects (CMIP): CMIP1 (Meehl *et al.* 2000) organized in the mid-1990s; CMIP2 (Covey *et al.* 2003, Meehl *et al.* 2005); and CMIP3 (PCMDI 2007) based on the IPCC Fourth Assessment Report (AR4, Meehl *et al.* 2007, Randall *et al.* 2007) simulations that were produced by the most-current climate models. For the calculation of the multivariate performance index, observations and global gridded analyses were used to compute annual-mean climatologies for the period 1979–1999. From this data set can be calculated errors in the modeled mean states of many different climate variables. To determine a model performance index, a normalized error variance,  $e^2$ , is calculated by squaring the grid-point differences between simulated and observed climate, normalizing for each grid point with the observed interannual variance, and averaging globally. This can be written as

$$e_{vm}^2 = \sum_n w_n (\bar{s}_{vmn} - \bar{o}_{vn})^2 / \sigma_{vn}^2,$$

where  $\bar{s}_{vmn}$  is the simulated annual climatological mean for variable  $v$ , model  $m$ , and grid point  $n$ ,  $\bar{o}_{vn}$  is the corresponding observed climatology;  $w_n$  are weights required for area and mass averaging; and  $\sigma_{vn}^2$  is the interannual variance based on the observations. One challenge when combining errors for variables with different dimensions is to weight them properly. In this method,  $e^2$  is scaled according to the average error for a reference ensemble of models. Specifically, a performance index ( $I$ ) is calculated as follows:

$$I_{vm}^2 = e_{vm}^2 / \overline{e_{vm}^2}^m,$$

where the overbar represents an average of the climates from all the models for that variable. The final step in calculating the performance index involves averaging over all the variables:

$$I_m^2 = \overline{I_{vm}^2}^v.$$

Figure 16.2 shows the value of the performance index,  $I_m^2$ , (solid vertical lines) for each of the models, for each of the three generations of CMIP exercises. The average performance index for each generation of models is shown by the dashed vertical line. The value of the index associated with the NCEP-NCAR reanalysis (Kalnay *et al.* 1996), which is a model-based analysis of observations, is 0.4. And, the black circle indicates the performance of the multi-model ensemble mean. The figure depicts a large variation in the ability

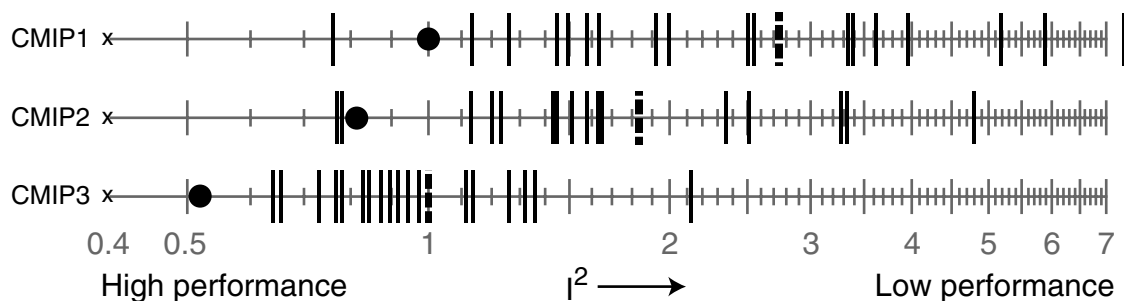


Fig. 16.2

Performance index,  $I^2$ , for individual models (vertical black lines) and model generations (CMIP1, CMIP2, and CMIP3).

The dashed vertical lines show the average performance index for each model generation, the  $\times$ 's at the left edge of the scales indicate the value of the performance index when the NCEP-NCAR reanalysis is used to define the climate, and the black solid circles show the performance index for the multi-model ensemble mean for each generation.

Better performing models have lower index values, to the left. Adapted from Reichler and Kim (2008).

of the models of a given generation to replicate the current climate. Also, there is a steady improvement in this ability from one generation to the next, such that the realism of the climate of the best models from CMIP3 approaches that of the atmospheric reanalysis. These generational improvements are at least partly a consequence of improvements in physical-process parameterizations and the greater horizontal and vertical resolution that has been permitted by increases in available computing capacity.

Another example of the relative performance of the individual models used in the Third IPCC Assessment Report (*c.* 2000), and those used in the current IPCC AR4, is provided in Randall *et al.* (2007) (Section 8.3.5). These statistics are reported individually for different variables, such as precipitation, sea-level pressure, and surface air temperature, rather than for a single performance index. Conclusions are that (1) on average, flux-adjusted models have smaller errors than those without flux adjustments, for both the third and fourth assessments, but the smallest errors are from models without flux adjustments; and (2) the mean error from the recent suite of models is smaller than that from the earlier suite, in spite of the fact that all but two of the newer models do not use flux adjustments.

An illustration of historical-temperature change produced by CMIP3 simulations is shown in Fig. 16.3. Depicted is the observed global-average near-surface temperature trace from 1900 to the early twenty-first century (black line), the simulations from the individual models used in the ensemble (light gray lines), and the multi-model ensemble mean (heavy gray line). The model simulations shown in Fig. 16.3a employed both natural and anthropogenic forcings, and those in Fig. 16.3b used only natural forcings. The ensemble-mean model-simulated temperature in Fig. 16.3a closely approximates the observed trend.

The relative skill of different models of an ensemble in replicating the observed historical climate can be used to infer which models will perform best for future climates. For example, Shukla *et al.* (2006) correlated the skill at simulating twentieth-century surface temperature with simulated future-climate temperatures. The models that had the smallest error for the twentieth-century climate produced relatively larger temperature increases for the twenty-first century. Meehl *et al.* (2007) describe the use of observation-based metrics

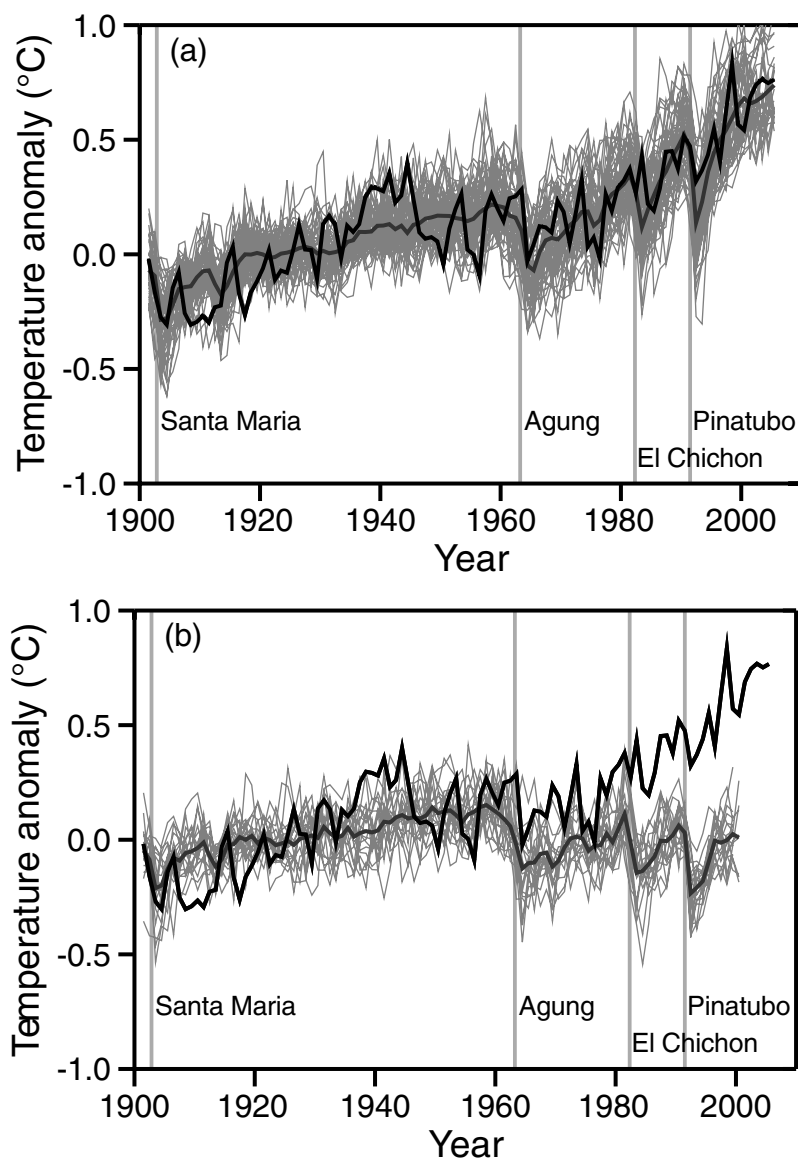


Fig. 16.3

Global-mean, near-surface temperature from observations (heavy black line) and from some of the individual climate models listed in Table 16.1 (light gray lines), based on the use in the models of (a) both natural and anthropogenic forcings and (b) natural forcings only. The temperature is represented as an anomaly relative to the observed 1900–1950 mean. The multi-model ensemble means are shown as relatively smooth heavy dark-gray lines. Vertical lines indicate the timing of major volcanic events. Adapted from Hegerl *et al.* (2007), which should be referenced for additional detail.

to weight the reliability of contributing models when making projections with ensembles, but a challenge is defining a metric, or a set of metrics, that is a reasonable indicator of overall model performance.

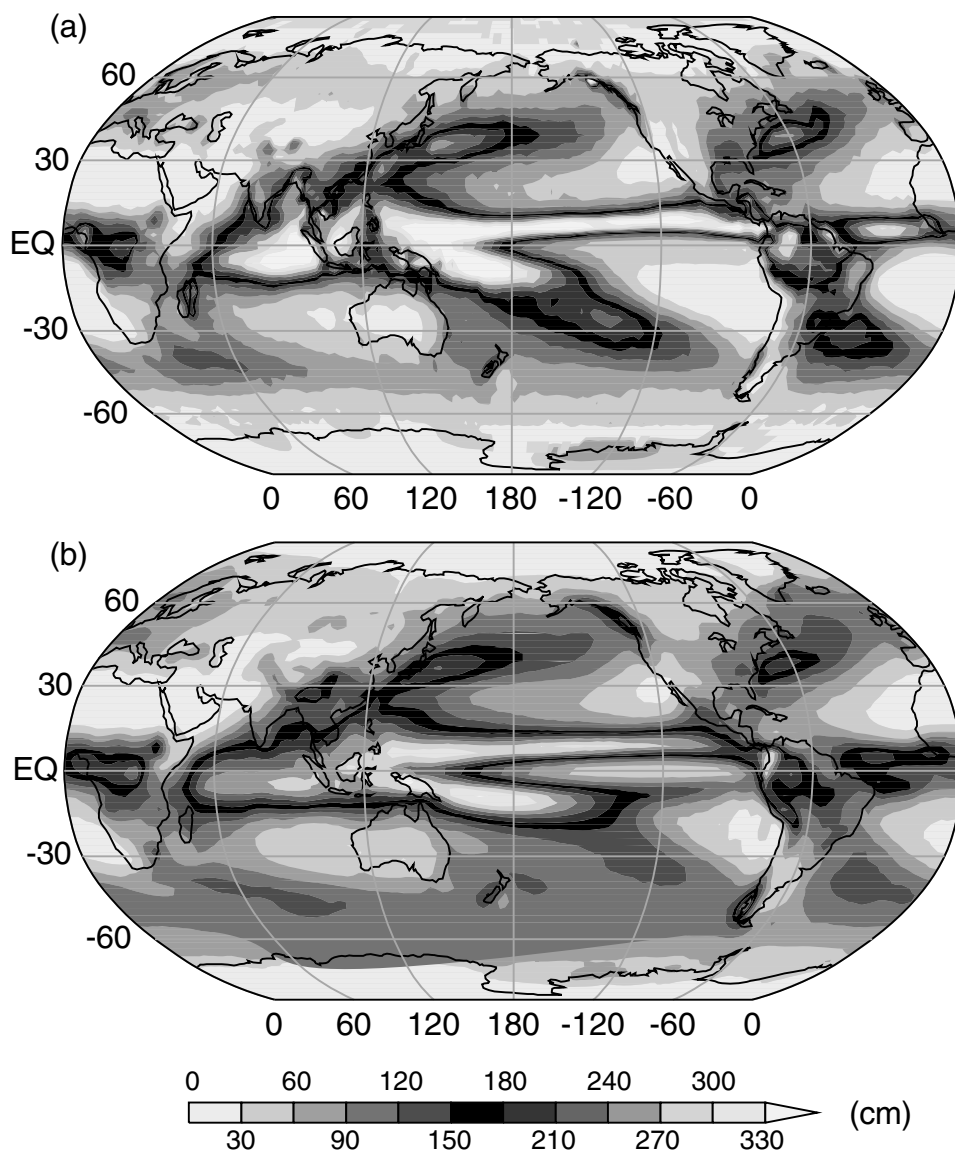
## Verification of specific processes and regional features

The above verification involved the calculation of global-average statistics, which facilitated the use of multivariate composite error indices. In contrast, this section provides examples of how global climate models have been evaluated (1) in the context of specific physical processes, such as the ENSO cycle, (2) in terms of the spatial pattern of error over the globe, and (3) for limited geographic areas. The inability of some climate models to faithfully simulate specific observed features of the current atmosphere has historically been the cause for a lack of confidence in the models for use in climate prediction.

As an example of the models' replication of spatial patterns, Fig. 16.4 shows the spatial distribution of annual-mean precipitation based on observations and CMIP3 climate-model simulations. The observation-based climatology is from the NOAA Climate Prediction Center (CPC) Merged Analysis of Precipitation (Xie and Arkin 1997) for the period 1980 to 1999. The model climate is based on a multi-model mean for the same period. The observed and simulated patterns are very similar, but quantitative differences are apparent regionally. For example, the subtropical precipitation deficits to the west of the continents in the Americas are less widespread and intense in the model solution, and the simulated precipitation maxima off the east coasts in midlatitudes are also smaller and weaker. An example of a more-quantitative interpretation of model skill at the regional level, also for precipitation, is provided in Fig. 16.5. It shows the annual cycle of regional-average precipitation for southwestern USA, simulated by the models participating in the CMIP2 comparison. Even though the overall cycle is captured, there is much variation among the models in the specific monthly precipitation values. AchutaRao *et al.* (2004) show similar plots for other variables and geographic areas.

There are many examples of studies that have focussed on the ability of climate models to simulate specific processes in the current climate. For example, precipitation is a primary climate variable, and in the tropics the diurnal cycle dominates its occurrence. However, many models have difficulty simulating the early-evening maximum, instead producing it before noon (Yang and Slingo 2001, Dai 2006). The ENSO cycle has been a process that has received special attention in terms of climate-model verification. For example, AchutaRao and Sperber (2006) compared the ENSO-simulation skill of the CMIP2 AOGCMs developed in the late 1990s with the skill of the more-recent models used as the basis for the IPCC AR4. The AR4 models were better in many respects, but the fact that fewer of those models use flux corrections may have prevented an otherwise greater improvement. Also, Randall *et al.* (2007) review progress with respect to the ability of climate models to simulate the Madden–Julian oscillation, the quasi-biennial oscillation, ENSO, and intraseasonal to interannual variability in monsoons. Also summarized is the ability of the models to reproduce observed extreme events in the current climate, including extreme temperatures, extreme precipitation events, and tropical cyclones.

The extreme values of model dependent variables, in new climate regimes, are often of equal or greater interest than are mean values. For example, greater temperature extremes associated with heat waves would take a larger toll in human lives, wind extremes would affect wind-power generation as well as the engineering design of tall buildings, heavier rains would produce more floods and flash floods that affect public safety, more-prolonged drought

**Fig. 16.4**

Annual-mean precipitation (cm) from an analysis of observations (a) and model simulations (b) for the period 1980–1999. The simulation is based on a CMIP3 multi-model mean and the analysis is a merger of gauge observations, satellite estimates, and model output. Adapted from Randall *et al.* (2007).

periods would have water-resources and agricultural implications, and stronger hurricanes would increase the loss of lives and infrastructure in coastal communities. Thus, there is a great emphasis in global and regional climate-change studies on verifying the model simulations of extremes for current climates and forecasting them for future climates. For example, a European project entitled Modeling the Impact of Climate Extremes (MICE) involved the use of both climate models and impact models (Hanson *et al.* 2007). Also, Meehl and Tebaldi

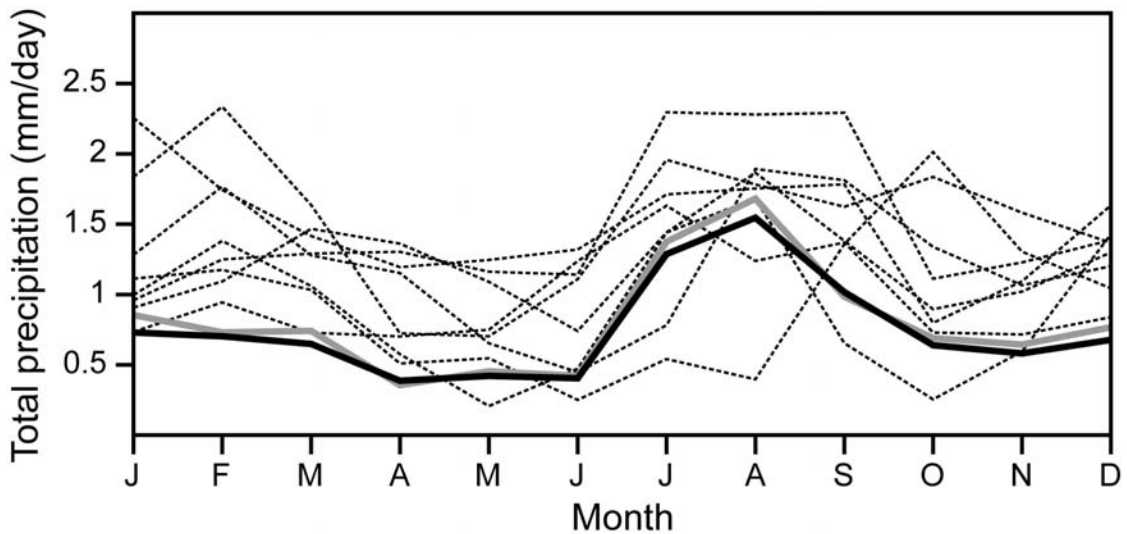


Fig. 16.5

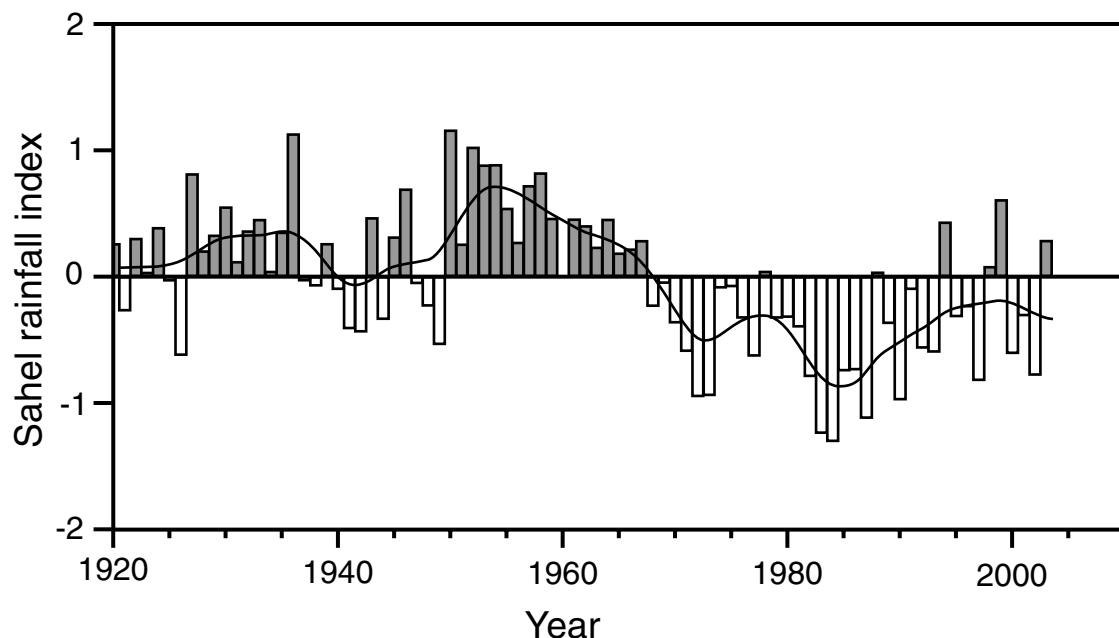
Monthly total precipitation for the southwest USA, based on the models participating in the CMIP-2 comparison (fine dashed lines), the precipitation analyses of Xie and Arkin (1996, 1997) (gray line), and the NOAA CPC Merged Analysis of Precipitation (CMAP) (wide black line). The region was defined by 30.0–37.5° N latitude and 105–115° W longitude. From AchutaRao *et al.* (2004).

(2004) use an ensemble of AOGCM predictions to conclude that heat waves in North America and Europe will become more intense, more frequent, and longer lasting in the second half of the twenty-first century. Additional examples of the use of ensembles for prediction of extremes are Alexander and Arblaster (2009) and Fowler and Ekström (2009).

#### 16.1.4 Seasonal to multi-year initial-value predictions

Regional climate variability on time scales of seasons to decades must be forecast in order to permit preparation for the economic, humanitarian, and environmental consequences of the change. Variability on these time scales can result from anthropogenic, greenhouse-gas forcing and from landscape changes, but also because of internal variability in the climate system. For example, Fig. 16.6 shows the Sahel-average precipitation record for a recent 83-year period, where there is evidence of variability on times scales of a few years to multiple decades. See Barnston and Livezey (1987) for a summary of the low-frequency atmospheric-circulation patterns. To forecast the internal variation, which results from the atmosphere's response to sea-surface temperatures, soil moisture, and snow and sea ice, the full physical system must be initialized. Kanamitsu *et al.* (2002b) suggests that there are at least four major requirements for a successful dynamical seasonal prediction system:

- accurate models of the atmosphere, ocean, land, and sea ice that are coupled in a physically consistent manner;
- initial conditions for the atmosphere, ocean, land, and sea ice;
- a methodology for ensemble prediction; and
- a strategy for correcting the systematic error.

**Fig. 16.6**

Time series of Sahel ( $10^{\circ}\text{N}$ – $20^{\circ}\text{N}$ ,  $18^{\circ}\text{W}$ – $20^{\circ}\text{E}$ ) regional rainfall during the rainy season (April–October) from 1920 through 2003, illustrating large changes on time scales of years to decades. Negative values of the index correspond to deficits relative to the period mean, and positive values are excesses. It is these changes, which include internal climate variability, that interseasonal to decadal predictions are designed to capture. The black curve shows decadal time-scale variations. From Trenberth *et al.* (2007).

Thus, the modeling system, in addition to encompassing the atmosphere, needs to also represent all the slower components of the variability in the system – the ocean, the land, and the ice. Defining the initial conditions for the forecasts is especially challenging because these slowly varying systems are not well-measured in three dimensions. Thus, data-assimilation systems must be relied upon, where the models themselves provide information that supplements the observations. And, as with longer-range simulations of greenhouse-gas emission scenarios, ensemble methods are important here. However, in addition to the multi-model ensemble methods used for simulation of those scenarios, the fact that this is an initial value problem with some poorly observed variables means that the initial-condition uncertainty must be sampled as well. Lastly, the model bias must be removed by subtracting the model climatology from the seasonal prediction to produce an anomaly field, and then adding the resulting anomaly to the observed climatology. This is equivalent to correcting the prediction using the difference between the model and observed climatology, and significantly increases the forecast skill of the model. A disadvantage of having to correct for this systematic error is that the error is a function of forecast lead times as well as month/season, and is best calculated through performing a large number of predictions with previous cases (reforecasts). Unfortunately, every time changes are made to the model, the systematic error must be recomputed. This problem is similar to the one described in Chapter 13 on the post processing of model output, where



the correction of weather forecasts using MOS precludes making frequent improvements and code corrections in the forecast model.

A number of special projects have been aimed at improving seasonal predictions. For example, the DEMETER project employed models from seven institutions in Europe. Using hindcasts, seasonal predictability was assessed for single-model ensembles, and for combining the single-model ensembles to produce multi-model superensembles. Palmer *et al.* (2004) and Hagedorn *et al.* (2005) summarize the project, and Doblas-Reyes *et al.* (2005) discuss the calibration of the ensemble and the combination of the members. A significant amount of the research effort related to prediction on these time scales has been focussed, understandably, on development and verification of methods for the prediction of the ENSO cycle (e.g., Gualdi *et al.* 2005, Keenlyside *et al.* 2005).

There are also seasonal climate-prediction methods that are based on a combination of dynamical and statistical models. For example, O'lenic *et al.* (2008) describe such a system used by the NCEP Climate Prediction Center for producing predictions with lead times of 1 month to 12 months. Also, there are research efforts that are aimed at extending the seasonal and multi-year initial-value prediction methods for use on time scales of decades (e.g., Smith *et al.* 2007, Keenlyside *et al.* 2008).

### 16.1.5 Summary of existing global models

#### Global models used for forced anthropogenic climate-change prediction

Table 16.1 lists the AOGCMs, from a variety of different research centers worldwide, that were involved in the IPCC AR4 (Randall *et al.* 2007). Most of the model versions originated in the late 1990s or the first five years of the twenty-first century. For the atmospheric models, the horizontal grid increments varied from about one degree (T106) to five degrees latitude–longitude, and the number of vertical levels varied from 12 to 56. The coupled ocean models typically had similar or better horizontal resolution than that of the corresponding atmospheric models, and the number of vertical ocean levels ranged from 16 to 47. Most of the models represent sea-ice rheology and leads in the ice. Only a few use flux adjustments. Lastly, regarding land-surface processes, most employ multi-layer soil models, route surface water in channels, and have some representation of a vegetation canopy. The main point of showing this table is to emphasize the tremendous effort that is being dedicated to the modeling of radiatively forced climate change.

#### Global models used for seasonal to multi-year initial-value predictions

Interseasonal prediction systems sometimes employ atmospheric models that are similar to the AGCMs that are used for medium-range forecasting, but a separately run ocean model provides the SSTs. For longer time-scale predictions, fully coupled AOGCMs are used. Interseasonal forecasts are produced operationally by a number of national centers, on a regular forecast cycle. Ensemble methods are virtually always employed. Table 16.2 lists some of the models that are being used operationally on seasonal to annual time scales.

**Table 16.1** Features of atmosphere–ocean general-circulation models used in the IPCC Fourth Assessment

<b>Model ID, Vintage</b>	<b>Sponsor(s), Country</b>	<b>Atmosphere</b> Top, Resolution, References	<b>Ocean</b> Resolution, z Coord., Top BC, References	<b>Sea ice</b> Dynamics, Leads, References	<b>Coupling flux adjustments</b> References	<b>Land, Soil, Plants</b> Routing, References
1. BCC-CM1 2005	Beijing Climate Center, China	top = 25 hPa T63 ( $1.9^\circ \times 1.9^\circ$ ) L16 CSMD 2005; Xu <i>et al.</i> 2005	$1.9^\circ \times 1.9^\circ$ L30 depth, free surface Jin <i>et al.</i> 1999	no rheology or leads Xu <i>et al.</i> 2005	heat, momentum Yu and Zhang 2000; CSMD 2005	layers, canopy, routing CSMD 2005
2. BCCR- BCM2.0 2005	Bjerknes Centre for Climate Research, Norway	top = 10 hPa T63 ( $1.9^\circ \times 1.9^\circ$ ) L31 Déqué <i>et al.</i> 1994	$0.5^\circ - 1.5^\circ \times 1.5^\circ$ L35 density, free surface Bleck <i>et al.</i> 1992	rheology, leads Hibler 1979; Harder 1996	no adjustments Furevik <i>et al.</i> 2003	layers, canopy, routing Mahfouf <i>et al.</i> 1995; Douvillie <i>et al.</i> 1995; Oki and Sud 1998
3. CCSM3 2005	National Center for Atmospheric Research, USA	top = 2.2 hPa T85 ( $1.4^\circ \times 1.4^\circ$ ) L26. Collins <i>et al.</i> 2004	$0.3^\circ - 1^\circ \times 1^\circ$ L40 depth, free surface Smith and Gent 2002	rheology, leads Briegleb <i>et al.</i> 2004	no adjustments Collins <i>et al.</i> 2006a	layers, canopy, routing Oleson <i>et al.</i> 2004; Branstetter 2001
4. CGCM3.1 (T47) 2005	Canadian Centre for Climate Modelling and Analysis	top = 1 hPa T47 ( $2.8^\circ \times 2.8^\circ$ ) L31 McFarlane <i>et al.</i> 1992	$1.9^\circ \times 1.9^\circ$ L29 depth, rigid lid Pacanowski <i>et al.</i> 1993	rheology, leads Hibler 1979; Flato and Hibler 1992	heat, fresh water	layers, canopy, routing Verseghy <i>et al.</i> 1993
5. CGCM3.1 (T63) 2005		top = 1 hPa T63 ( $1.9^\circ \times 1.9^\circ$ ) L31 McFarlane <i>et al.</i> 1992	$0.9^\circ \times 1.4^\circ$ L29 depth, rigid lid Flato and Boer 2001; Kim <i>et al.</i> 2002	rheology, leads Hibler 1979; Flato and Hibler 1992	heat, fresh water	layers, canopy, routing Verseghy <i>et al.</i> 1993
6. CNRM- CM3 2004	Météo-France/ Centre National de Recherches Météorologiques, France	top = 0.05 hPa T63 ( $1.9^\circ \times 1.9^\circ$ ) L45 Déqué <i>et al.</i> 1994	$0.5^\circ - 2^\circ \times 2^\circ$ L31 depth, rigid lid Madec <i>et al.</i> 1998	rheology, leads Hunke and Dukowicz 1997; Salas-Mélia 2002	no adjustments Terray <i>et al.</i> 1998	layers, canopy, routing Mahfouf <i>et al.</i> 1995; Douvillie <i>et al.</i> 1995; Oki and Sud 1998

**Table 16.1** (continued)

Model ID, Vintage	Sponsor(s), Country	Atmosphere Top, Resolution, References	Ocean Resolution, z Coord., Top BC, References	Sea ice Dynamics, Leads, References	Coupling flux adjustments References	Land, Soil, Plants Routing, References
7. CSIRO-MK3.0 2001	Commonwealth Scientific and Industrial Research Organisation, Australia	top = 4.5 hPa T63 ( $1.9^\circ \times 1.9^\circ$ ) L18 Gordon <i>et al.</i> 2002	$0.8^\circ \times 1.9^\circ$ L31 depth, rigid lid Gordon <i>et al.</i> 2002	rheology, leads O'Farrell 1998	no adjustments Gordon <i>et al.</i> 2002	layers, canopy Gordon <i>et al.</i> 2002
8. CHAMS/ MPI-OM 2005	Max Planck Inst. for Meteorology, Germany	top = 10 hPa T63 ( $1.9^\circ \times 1.9^\circ$ ) L31 Roeckner <i>et al.</i> 2003	$1.5^\circ \times 1.5^\circ$ L40 depth, free surface Marsland <i>et al.</i> 2003	rheology, leads Hibler 1979; Semtner 1976	no adjustments Jungclaus <i>et al.</i> 2006	bucket, canopy, routing Hagemann 2002; Hagemann and Dümenil-Gates 2001
9. ECHO-G 1999	Meteorological Institute of the University of Bonn, Meteorological Research Institute of the Korea Meteorological Administration, and Model and Data Group, Germany/ Korea	top = 10 hPa T30 ( $3.9^\circ \times 3.9^\circ$ ) L19 Roeckner <i>et al.</i> 1996	$0.5^\circ - 2.8^\circ \times 2.8^\circ$ L20 depth, free surface Wolff <i>et al.</i> 1997	rheology, leads Wolff <i>et al.</i> 1997	heat, fresh water Min <i>et al.</i> 2005	bucket, canopy, routing Roeckner <i>et al.</i> 1996; Dümenil and Todini 1992
10. FGOALS-g1.0 2004	National Key Laboratory of Numerical Modeling for Atmospheric Science and Geophysical Fluid Dynamics/Institute of Atmospheric Physics, China	top = 2.2 hPa T42 ( $2.8^\circ \times 2.8^\circ$ ) L26 Wang <i>et al.</i> 2004	$1.0^\circ \times 1.0^\circ$ L16 eta, free surface Jin <i>et al.</i> 1999; Liu <i>et al.</i> 2004	rheology, leads Briegleb <i>et al.</i> 2004	no adjustments Yu <i>et al.</i> 2002, 2004	layers, canopy, routing Bonan <i>et al.</i> 2002

11. GFDL-CM2.0 2005	U.S. Department of Commerce/National Oceanic and Atmospheric Administration/Geophysical Fluid Dynamics Laboratory, USA	top = 3 hPa $2.0^\circ \times 2.5^\circ$ L24 GFDL GAMDT 2004	$0.3^\circ - 1.0^\circ \times 1.0^\circ$ depth, free surface Gnanadesikan <i>et al.</i> 2006	rheology, leads Winton 2000; Delworth <i>et al.</i> 2006	no adjustments Delworth <i>et al.</i> 2006	bucket, canopy, routing Milly and Shmakin 2002; GFDL GAMDT 2004
12. GFDL-CM2.1 2005		top = 3 hPa $2.0^\circ \times 2.5^\circ$ L24 GFDL GAMDT 2004 with semi-Lagrangian transports	$0.3^\circ - 1.0^\circ \times 1.0^\circ$ depth, free surface Gnanadesikan <i>et al.</i> 2006	rheology, leads Winton 2000; Delworth <i>et al.</i> 2006	no adjustments Delworth <i>et al.</i> 2006	bucket, canopy, routing Milly and Shmakin 2002; GFDL GAMDT 2004
13. GISS-AOM 2004	National Aeronautics and Space Administration (NASA)/Goddard Institute for Space Studies (GISS), USA	top = 10 hPa $3^\circ \times 4^\circ$ L12 Russell <i>et al.</i> 1995	$3^\circ \times 4^\circ$ L16 mass/area, free surface Russell <i>et al.</i> 1995	rheology, leads Flato and Hibler 1992	no adjustments	layers, canopy, routing Abramopoulos <i>et al.</i> 1988; Miller <i>et al.</i> 1994
14. GISS-EH 2004		top = 0.1 hPa $4^\circ \times 5^\circ$ L20 Schmidt <i>et al.</i> 2006	$2^\circ \times 2^\circ$ L16 density, free surface Bleck 2002	rheology, leads Liu <i>et al.</i> 2003; Schmidt <i>et al.</i> 2004	no adjustments Schmidt <i>et al.</i> 2006	layers, canopy, routing Friend and Kiang 2005
15. GISS-ER 2004	NASA/GISS, USA	top = 0.1 hPa $4^\circ \times 5^\circ$ L20 Schmidt <i>et al.</i> 2006	$4^\circ \times 5^\circ$ L13 mass/area, free surface Russell <i>et al.</i> 1995	rheology, leads Liu <i>et al.</i> 2003; Schmidt <i>et al.</i> 2004	no adjustments Schmidt <i>et al.</i> 2006	layers, canopy, routing Friend and Kiang 2005
16. INM-CM3.0 2004	Institute for Numerical Mathematics, Russia	top = 10 hPa $4^\circ \times 5^\circ$ L21 Galin <i>et al.</i> 2003	$2^\circ \times 2.5^\circ$ L33 sigma, rigid lid Diansky <i>et al.</i> 2002	no rheology or leads Diansky <i>et al.</i> 2002	regional fresh water Diansky and Volodin 2002; Volodin and Diansky 2004	layers, canopy, no routing Volodin and Lykosoff 1998
17. IPSL-CM4 2005	Institute Pierre Simon Laplace, France	top = 4 hPa $2.5^\circ \times 3.75^\circ$ L19 Hourdin <i>et al.</i> 2006	$2^\circ \times 2^\circ$ L31 depth, free surface Madec <i>et al.</i> 1998	rheology, leads Fichefet and Morales-Maqueda 1997; Goosse and Fichefet 1999	no adjustments Marti <i>et al.</i> 2005	layers, canopy, routing Krinner <i>et al.</i> 2005

**Table 16.1** (continued)

Model ID, Vintage	Sponsor(s), Country	Atmosphere Top, Resolution, References	Ocean Resolution, z Coord., Top BC, References	Sea ice Dynamics, Leads, References	Coupling flux adjustments References	Land, Soil, Plants Routing, References
18. MIROC3.2 (hires) 2004	Center for Climate System Research (University of Tokyo), National Institute for Environmental Studies, and Frontier Research Center for Global Change, Japan	top = 40 km T106 ( $1.1^\circ \times 1.1^\circ$ ) L56 K-1 Developers 2004	$0.2^\circ \times 0.3^\circ$ L47 sigma/depth, free surface K-1 Developers 2004	rheology, leads K-1 Developers 2004	no adjustments K-1 Developers 2004	layers canopy, routing K-1 Developers 2004; Oki and Sud 1998
19. MIROC3.2 (medres) 2004		top = 30 km T42 ( $2.8^\circ \times 2.8^\circ$ ) L20 K-1 Developers 2004	$0.5^\circ\text{--}1.4^\circ \times 1.4^\circ$ L43 sigma/depth, free surface K-1 Developers 2004	rheology, leads K-1 Developers 2004	no adjustments K-1 Developers 2004	layers, canopy, routing K-1 Developers 2004; Oki and Sud 1998
20. MRI- CGCM 2.3.2 2003	Meteorological Research Institute, Japan	top = 0.4 hPa T42 ( $2.8^\circ \times 2.8^\circ$ ) L30 Shibata <i>et al.</i> 1999	$0.5^\circ\text{--}2.0^\circ \times 2.5^\circ$ L23 depth, rigid lid Yukimoto <i>et al.</i> 2001	free drift, leads Mellor and Kantha 1989	heat, fresh water, momentum ( $12^\circ\text{S--}12^\circ\text{N}$ ) Yukimoto <i>et al.</i> 2001	layers, canopy, routing Sellers <i>et al.</i> 1986; Sato <i>et al.</i> 1989
21. PCM 1998	National Center for Atmospheric Research, USA	top = 2.2 hPa T42 ( $2.8^\circ \times 2.8^\circ$ ) L26 Kiehl <i>et al.</i> 1998	$0.5^\circ\text{--}0.7^\circ \times 1.1^\circ$ L40 depth, free surface Maltrud <i>et al.</i> 1998	rheology, leads Hunke and Dukowicz 1997, 2003; Zhang <i>et al.</i> 1999	no adjustments Washington <i>et al.</i> 2000	layers, canopy, no routing Bonan 1998
22. UKMO- HadCM3 1997	Hadley Centre for Climate Prediction and Research/Met Office, UK	top = 5 hPa $2.5^\circ \times 3.75^\circ$ L19 Pope <i>et al.</i> 2000	$1.25^\circ \times 1.25^\circ$ L20 depth, rigid lid Gordon <i>et al.</i> 2000	free drift, leads Cattle and Crossley 1995	no adjustments Gordon <i>et al.</i> 2000	layers, canopy, routing Cox <i>et al.</i> 1999
23. UKMO- HadGEM1 2004		top = 39.2 km $1.3^\circ \times 1.9^\circ$ L38 Martin <i>et al.</i> 2004	$1.0^\circ \times 1.0^\circ$ L40 depth, free surface Roberts 2004	rheology, leads Hunke and Dukowicz 1997; Semtner 1976; Lipscomb 2001	no adjustments Johns <i>et al.</i> 2006	layers, canopy, routing Oki and Sud 1998

Source: Adapted from Randall *et al.* (2007).

The first column shows the IPCC identification, with the calendar year of the first publication describing the model results. The second column lists the sponsoring institution and country. The third shows the pressure at the top boundary of the model, the horizontal resolution in terms of the spectral truncation and/or the latitude–longitude grid increment, and the number of vertical levels. The next column lists the horizontal grid increment of the ocean model, the number of computational levels, and the upper boundary condition. The fifth column shows information about sea-ice dynamics, and the sixth indicates whether there are flux adjustments to the interaction of the atmosphere and ocean. The last column lists properties of the land-surface model (soil, vegetation, water). The references listed should be consulted for more information.

**Table 16.2** Example global models used for operational seasonal to annual initial-value predictions. Note that forecast systems that combine dynamical and statistical models are not listed here.

Models (where model developed)	Organization producing forecast	Duration of predictions	References
CFS	NCEP	9 months	Saha <i>et al.</i> 2006
ECHAM (MPI)	IRI	6+ months	Barnston <i>et al.</i> 2003
CCSM (NCAR)			
MRF (NCEP)			
NSIPP (NASA)			
COLA			
ECPC (Scripps)			
System-III	ECMWF	3 months 1 year	Anderson <i>et al.</i> 2003 George and Sutton 2006
GloSea	UK Met Office	3 months	Gordon <i>et al.</i> 2000 Graham <i>et al.</i> 2005

Longer-range (decadal) initial-value predictions are performed on a one-time basis, rather than on a regular cycle. Even though the model products are used for development of adaptation strategies, the modeling is more reasonably defined as a research project rather than being operational.

### 16.1.6 Ensemble climate simulation

The use of ensemble methods in weather prediction is discussed in Chapter 7. The application of similar techniques has also been well established for seasonal, interannual, decadal, and centennial forecasting with AOGCMs. Good summaries are provided in Section 10.5.4 in Meehl *et al.* (2007). In contrast to ensemble weather prediction, predictions of forced anthropogenic climate change and inter-seasonal forecasting, both with AOGCMs, require the sampling of additional sources of uncertainty. For initial-value simulations, the uncertain initial state of the ocean and other components of the system must be sampled. For IPCC-type simulations, future emissions of aerosols and greenhouse gases are unknown, and this uncertainty can be sampled by assuming different scenarios. Also, ensembles can take two forms. In one, the same model can be used for multiple experiments with different choices for poorly constrained internal parameters and for the overall process parameterizations themselves. In the other, multi-model ensembles can be generated through the use of a range of AOGCMs developed at different modeling centers, such as used in the CMIP experiments described above or in the IPCC ensemble.

In experiments that define the climate response to different forcing scenarios, the change between the present state of a variable and the state in some future year is a result of both the start and end times. Because the aim of such experiments is to assess the impact of the forcing on the climate, it is typical to create an ensemble using different

initial times within the current climate, and use the average of the projections in order to minimize the influence of the internal variations.

To the degree that the errors from different AOGCMs used in an ensemble are independent of each other, the ensemble mean can be expected to outperform the individual ensemble members. Palmer *et al.* (2004), Hagedorn *et al.* (2005), and Krishnamurti *et al.* (2006b) demonstrate that this is the case for seasonal prediction. For longer-range radiatively forced scenarios, Lambert and Boer (2001), Taylor *et al.* (2004), and Reichler and Kim (2008) show the superiority of the ensemble mean over the use of individual members (e.g., Fig. 16.2). Indeed, the conclusions about global warming reported by the IPCC were based on the multi-model ensemble mean of the CMIP3 models.

As with ensemble weather prediction, ensemble climate predictions can be calibrated (Doblas-Reyes *et al.* 2005). Because of the disparate nature of the multi-national suite of climate models, it is not possible to make the assumption that all the models are equally skillful at predicting each variable at each geographic location. Thus, the optimal solution would not be based on an equally weighted combination of the model solutions. It was noted earlier that models that have verified better against the historical climate record may be given more weight in terms of their projections of future climate (e.g., Krishnamurti *et al.* 1999, Shukla *et al.* 2000, 2006, Goddard *et al.* 2001, Rajagopalan *et al.* 2002, Robertson *et al.* 2004, Yun *et al.* 2005). Clemen (1989) reviews different methods for optimally combining multi-model ensemble climate predictions.

One of the many examples of the benefits of ensemble climate prediction is described in Feddersen and Andersen (2005), who compared the skill of 2-month (seasonal) statistically downscaled multi-model ensemble predictions with the skill of the downscaled individual-model predictions. This comparison was made for 40 years of retrospective seasonal-forecast downscalings over Europe, northwest North America, the contiguous USA, Australia, and Scandinavia. The forecasts employed were part of the DEMETER study, and were performed by Météo-France, ECMWF, and the UK Meteorological Office (Palmer *et al.* 2004). A linear-regression-based downscaling algorithm was constructed using the ensemble mean from the model forecasts (the MOS approach mentioned in Section 16.3.1) and observations from the noted geographic areas. Using a cross-validation approach (Michaelsen 1987), the statistical relationship used in each forecast year was constructed without data from that year. The regression equation obtained from using the ensemble mean was also applied to the downscaling of the individual ensemble members. Table 16.3 shows the verification of the 2-month forecasts in terms of the anomaly correlation, for the individual models as well as the multi-model ensemble, for selected seasons and geographic areas. The predictive skill varies geographically, with season, and with the model. No single model is consistently better than another. The ensemble skill is generally comparable to that of the best model, where the positive scores indicate modest predictive skill beyond that of climatology. The skill varies from year to year, as seen in Fig. 16.7, which shows the time series of the anomaly correlation for the 2-m temperature for Europe in the JAS season. In years where the ensemble prediction shows no skill (negative or zero anomaly correlation), two of the member forecasts have typically failed. In most years, the anomaly correlation of the ensemble prediction is positive.



**Table 16.3** Comparison of the anomaly correlation for individual models and for the ensemble mean, for selected seasons and geographic regions.

Model	Precipitation		2-m Temperature	
	Europe JFM	Scandinavia JFM	Europe JAS	Scandinavia AMJ
Météo-France	0.07	0.11	0.16	0.33
ECMWF	0.30	0.09	0.35	0.14
UK Met Office	0.03	0.28	0.25	0.15
Ensemble	0.22	0.27	0.35	0.28

Source: From Feddersen and Andersen (2005).

Another European ensemble climate-prediction effort is ENSEMBLES (Hewitt 2005). This project involves the development, verification, and application of several AOGCMs and regional models to produce ensemble forecasts on time scales of seasons to decades. In addition to generating the probabilistic forecasts for Europe, the project is linking the outputs with the needs of various sectors such as agriculture, health, energy, water, and food security.

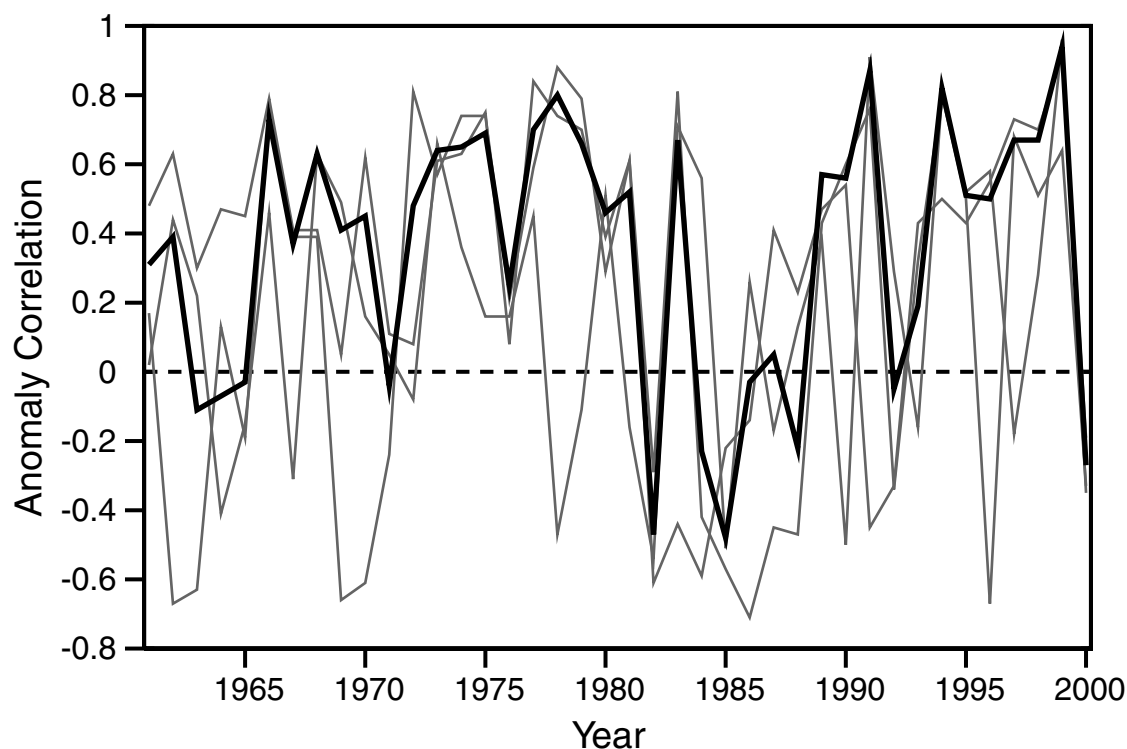


**Fig. 16.7** Anomaly correlations for 2-month downscaled predictions of 2-m temperature for JAS in Europe, averaged by year, for three models (thin lines) and for the ensemble mean (thick line). From Feddersen and Andersen (2005).

### 16.1.7 Example global climate-change predictions

Predictions with AOGCMs have been conducted on seasonal, annual, decadal, and centennial time scales. Even though our focus in this text is not on the results, but rather on the methods, a couple of examples will be provided of climate change that has been simulated by radiative-forcing experiments. Figure 16.8 illustrates the change in global-average surface air temperature and precipitation predicted for the twenty-first century by 21 AOGCMs used in the IPCC AR4 experiments. There is a significant spread among the model predictions, especially for precipitation, but all of the simulations have the same general trend. Of more direct use for addressing practical questions about adaptation to climate change are regional interpretations of the global-model output. Such regional analyses of the results of IPCC-ensemble simulations have been generated for a wide range of applications related to water resources, air quality, etc. For example, Fig. 16.9 shows the ensemble-mean predicted precipitation change in the Middle East between 2005 and 2050, based on 18 global climate models that participated in the IPCC AR4. These results indicate a trend toward a drier future to the north and east of the Mediterranean, along the track of extratropical cyclones. By the end of the century (not shown), the precipitation decrease exceeds 100 mm, and the temperature increases by 4 °C. Note that these types of regional analyses are not based on downscalings, but are simply windows within which the global-model output is displayed and analyzed. For other examples of regional analyses of AOGCM climate projections, see Gibein and Déqué (2003), Déqué *et al.* (2005), Cook and Vizy (2006), d'Orgeval *et al.* (2006), García-Morales and Dubus (2007), and Hanson *et al.* (2007).

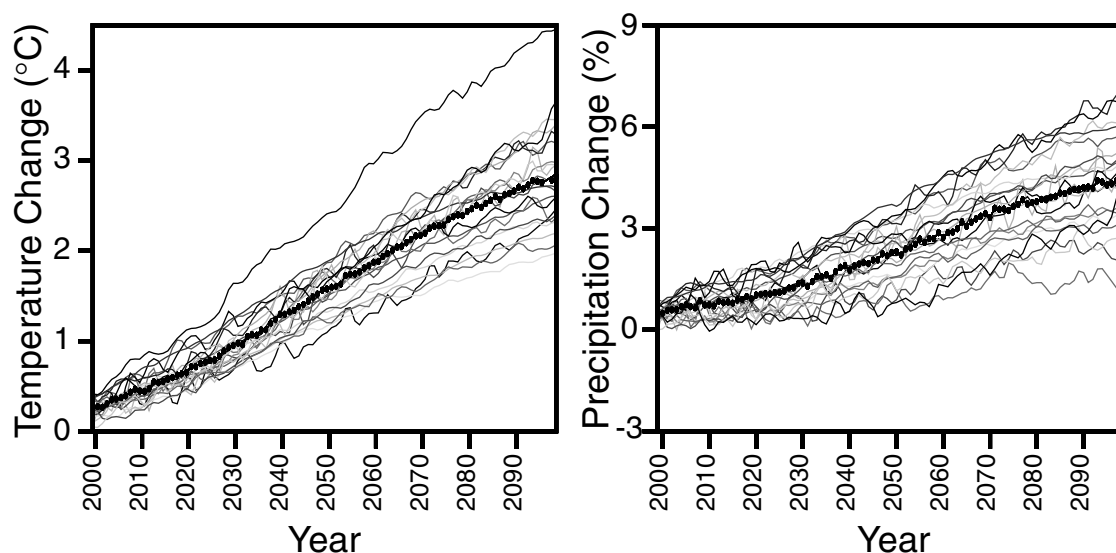


Fig. 16.8

Time series of globally averaged surface-temperature change (left) and precipitation change (right) for 21 AOGCMs employed in the IPCC AR4, for the A1B emissions scenario. The values plotted are annual means, relative to the 1980 to 1999 average from the corresponding twentieth century simulations. The multi-model ensemble means are plotted as black dots and the individual simulations are shown by the fine lines. From Meehl *et al.* (2007).

2050 - 2005

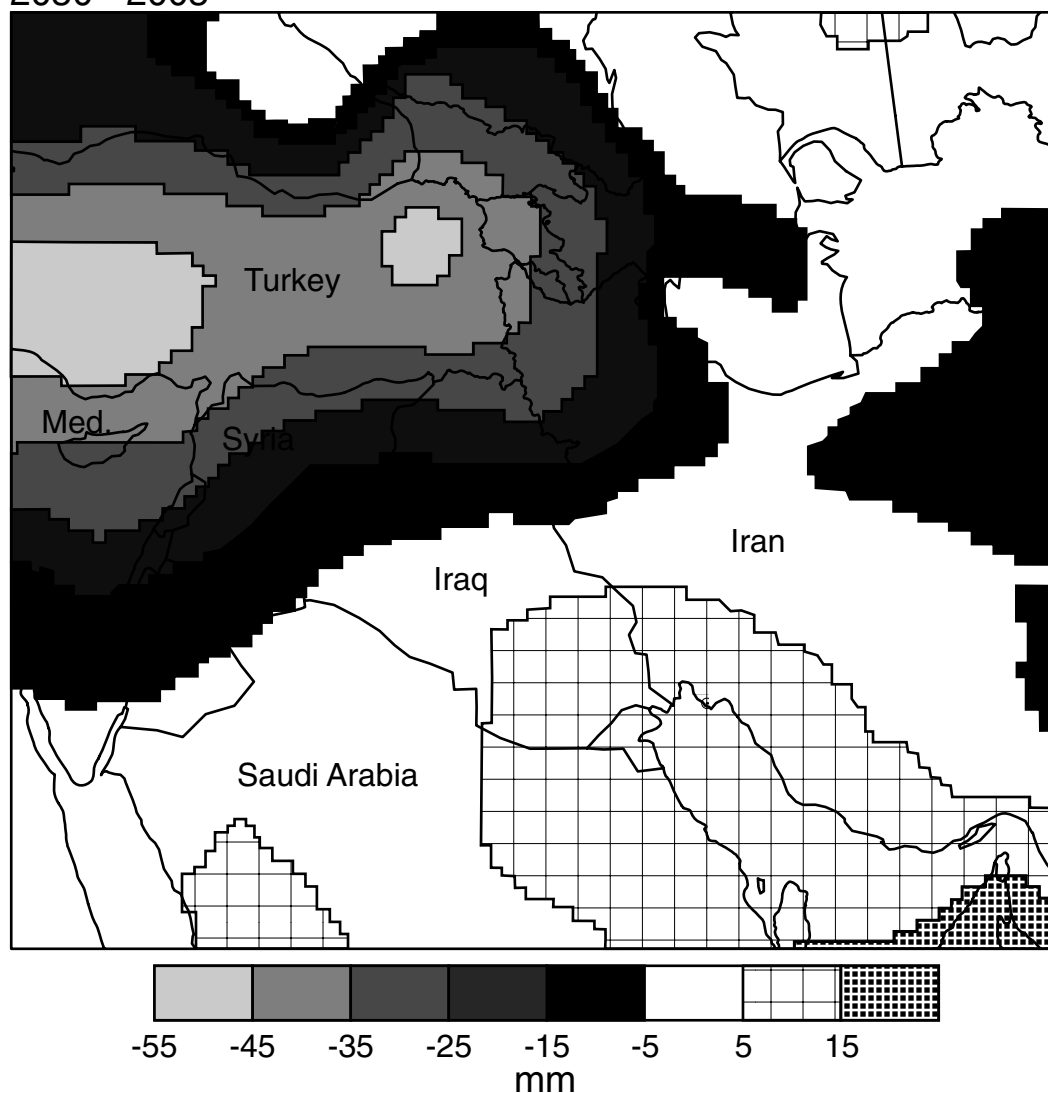


Fig. 16.9

Change in precipitation (mm) in the Middle East during the period 2005–2050, based on the ensemble mean of the predictions of 18 global models that participated in the IPCC AR4. Adapted from Evans (2008).

## 16.2 Reanalyses of the current global climate

Global data-assimilation systems typically employ a model to periodically ingest observations, with the result being a gridded set of model dependent variables that are consistent with both model dynamics and the information represented in the observations. The resulting analyses are sometimes called Model-Assimilated Data Sets (MADS). Such data-assimilation systems are used to define long-term analyses of atmospheric fields pertaining

to the current and recent climates, for use by the research and climate-monitoring communities, and they are used to provide initial conditions for operational GCM forecasts. The former process of reconstructing historical conditions involves using a contemporary, frozen version of the assimilation system, to generate multi-decadal analyses. These gridded data sets are called reanalyses.

Even though the same assimilation modeling software is used for the entire reanalysis period, to avoid any shifts in analyzed climate that would result from model changes, the types and amounts of ingested data obviously do change during the reanalysis period. Observation locations change, periodic data voids occur throughout entire nations or regions for political and economic reasons, and observation platforms such as satellites change throughout the period. Thus, there is an unavoidable lack of uniformity in the process that can lead to changes in the accuracy of the reanalysis and to difficulties in interpreting the climate. When major new observation platforms are introduced, parallel assimilations are run for short test periods, with and without the new data, to help isolate the impact of the new data on the analyzed climate.

Different analyzed variables have different relative dependencies on the model and assimilated observations. For example, surface fluxes and precipitation are often not assimilated, so their values provided in the reanalysis data set can be entirely products of the model. In contrast, winds, mass-field variables, and thermodynamic variables are assimilated, so the resulting analysis will represent a mix of the constraints of the observations and model dynamics.

The assimilation methods used in the different global reanalysis systems are similar. The NCEP-NCAR Reanalysis Project (NNRP) reanalysis (referred to as R-1, Kalnay *et al.* 1996) was generated with a 6-h intermittent-assimilation method, for the 40-year period from 1957 to 1996, using the NCEP Global Data-Assimilation System (Kanamitsu 1989, Kanamitsu *et al.* 1991). Here, an objective analysis is performed every 6 h, using the previous 6-h forecast as the first guess. The horizontal grid increment of the model and the analysis is about 210 km, and there are 28 layers in the vertical. An updated reanalysis was subsequently produced, with the same data input and model resolution, but with some model and data errors corrected (the NCEP-DOE Reanalysis, or R-2; Kanamitsu *et al.* 2002a). A more-recent global reanalysis is the ERA-40, also a second-generation product, produced by the ECMWF (Uppala *et al.* 2005). The assimilation model also used a 6-h assimilation cycle, the horizontal grid increment was about 125 km, and there were 60 layers in the vertical. Other global reanalyses are the Japanese 25-year Reanalysis Project (JRA-25, Onogi *et al.* 2007) and NASA's Modern Era Retrospective-analysis for Research and Applications (MERRA, Bosilovich *et al.* 2006). The MERRA analysis is defined on a 2/3 degree longitude by 1/2 degree latitude grid, with 72 vertical layers. The JRA-25 analysis has a horizontal grid size of about 120 km and 40 vertical layers.

## 16.3 Climate downscaling

The term *future-climate downscaling* refers to techniques that use AOGCM predictions of future climates as input to methods that produce finer-scale climate information. This

process is necessitated by the fact that the AOGCMs that are used for predicting future climate typically have grid spacings of hundreds of kilometers, and thus there is a mismatch between the output data of those models and the needs of, for example, hydrological models that require watershed-scale information. In the process of determining the accuracy of the AOGCMs and the downscaling methods, simulations of current or past climates may be performed, but the ultimate objective in future-climate downscaling studies is to produce high-horizontal-resolution information about future climates. Downscaling methods can be applied to initial-value-based interseasonal or longer forecasts, or to radiatively forced IPCC-type simulations.

There is also a need for gridded, high-horizontal-resolution information about the current climate. For example, wind-energy prospecting and defining source–receptor relationships in air-quality studies benefit from the availability of high-resolution mesoscale data that define the characteristics of the current climate. To satisfy this need, *current-climate downscaling* uses global gridded data sets that are produced by the global-model-based data-assimilation systems described in the last section.

For both present and future climates, there are two basic approaches for accomplishing this downscaling. One is to use statistical-empirical relationships that define the high-resolution subgrid-scale variability based on resolved, grid-scale, values from the global data set. The other uses a LAM whose LBCs are forced by the global data set, or a stretched-grid AGCM. The former process is referred to as *statistical downscaling*, while the latter is called *dynamical downscaling*. The advantages and disadvantages of the two approaches are summarized in Table 16.4.

Topics that are related to the subject of climate downscaling appear elsewhere in this book. For example, Chapter 13 about the post processing of model output discusses statistical downscaling as applied to weather prediction. And, the subject of forcing the LBCs of LAMs with global analyses or global forecast-model output is described in Chapter 3 on numerical methods.

Downscaling, whether it is statistically or dynamically based, is a local diagnostic process that represents a post processing of the global data set. That is, the modulations of the large-scale climate by local forcing, such as orography, are diagnosed by statistical or dynamical methods, but they typically cannot feed back to the global scales to improve the rendering of the climates of other regions. The exception is when variable-resolution global climate models focus higher horizontal resolution over certain geographic areas (discussed in Laprise 2008). Even in this latter situation, there are concerns that teleconnections between two distant geographic areas cannot be treated properly in climate simulations if only one region is modeled with high resolution. For example, if we are modeling the future climate of the Amazon Basin, we would be tempted to represent only that area with higher resolution. However, there is recent evidence (Koren *et al.* 2006) that the dust originating in the relatively small Bodélé Depression in the Sahara Desert provides a large fraction of the nutrients for Amazon vegetation. Thus, inadequate resolution of the orographically generated high winds in this area of Africa could lead to an erroneous devegetation of the Amazon in a future-climate simulation that was able to represent the effects of soil nutrients on the vegetation. Unfortunately, we often don't have sufficient understanding of the current climate

**Table 16.4** Summary of advantages and disadvantages of statistical and dynamical downscaling for current and future climates

	Statistical downscaling	Dynamical downscaling
<b>Advantages</b>	<ul style="list-style-type: none"> <li>• Computationally efficient, and cheap</li> <li>• Can be used to derive variables not available from RCMs (e.g., river discharge)</li> <li>• Easily transferable between different regions</li> <li>• Based on standard and accepted statistical procedures</li> <li>• Able to directly incorporate observations</li> <li>• Can provide climate variables at a point, based on large-scale input</li> </ul>	<ul style="list-style-type: none"> <li>• Response is based on physically consistent process</li> <li>• Gridded output is available for physical-process analysis</li> <li>• Can better capture extreme events and variance</li> </ul>
<b>Disadvantages</b>	<ul style="list-style-type: none"> <li>• Requires long and reliable observed historical data record for calibration</li> <li>• Success dependent upon choice of predictors</li> <li>• Nonstationarity may exist in the predictor–predictand relationship</li> <li>• Climate-system feedbacks not included</li> <li>• Variance is underestimated, may poorly represent extreme events</li> <li>• GCM biases can cause error, unless the procedure corrects for them</li> <li>• Domain size, region, and season affect skill</li> </ul>	<ul style="list-style-type: none"> <li>• Computationally intensive</li> <li>• Sensitive to location of lateral boundaries</li> <li>• Feedback to large scale generally not considered</li> <li>• Biases in large-scale conditions will cause errors</li> <li>• Domain size, region, and season affect skill</li> </ul>

sensitivities, such as the one just mentioned, let alone teleconnections that will be potentially important in future climates.

Section 16.1.3 describes the need for global climate models to provide information on the extremes in the PDFs of the dependent variables, for use in analyzing both current and future climates. Because atmospheric extremes tend to be associated with small-scale features, such as convective events, strong fronts, terrain-induced downslope winds, etc., it is understandable that coarse-resolution global-model-based analyses or predictions will tend to underestimate extremes, resulting in overly smooth features in analyses of the current climate or predictions of future climates. Thus, there has been much research activity associated with capturing the extremes with the downscaling process. For example, the STAtistical and Regional dynamical Downscaling of EXtremes (STARDEX) project was designed to compare statistical and dynamical downscaling methods in terms of their ability to estimate the extremes, for European future climates. For more information about STARDEX and the downscaling of extremes, see Fowler *et al.* (2007) and references therein. Figure 16.10 shows how downscaling with a Regional Climate Model (RCM) can better define extremes, by comparing the maximum one-day rainfall at a location in

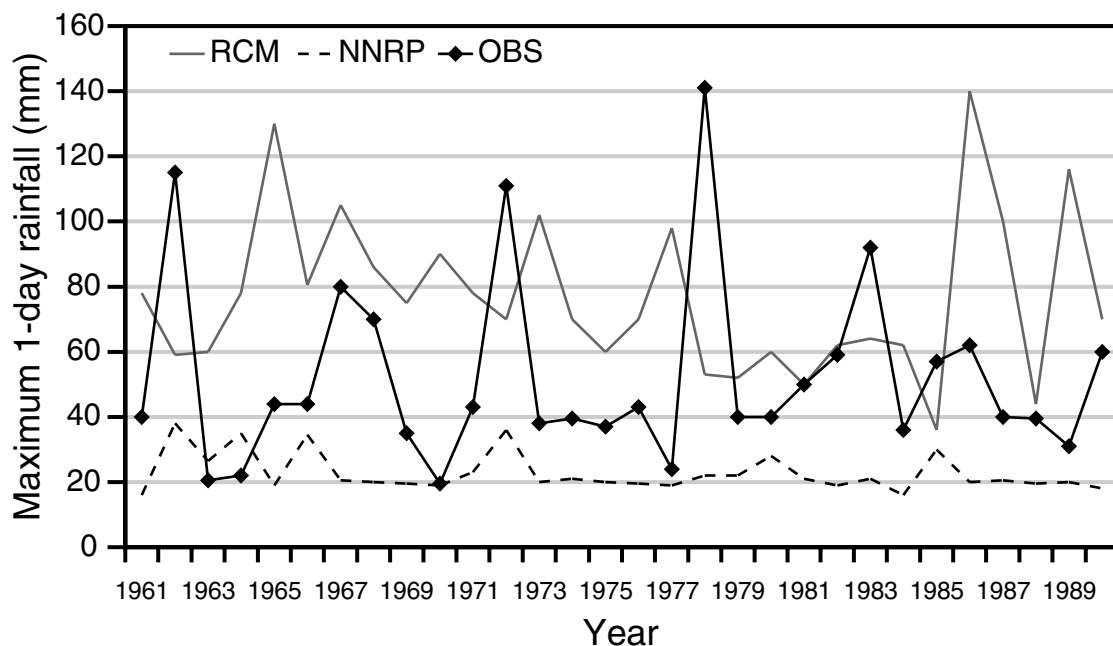


Fig. 16.10

Maximum one-day rainfall for Larissa, Greece, for each year of a 30-year period, based on the NNRP global-model-based reanalysis (NNRP), a downscaling simulation with the HadRM3 RCM (RCM), and rain-gauge observations (OBS). From Hanson *et al.* (2007).

Europe in each year of a 30-year period, based on observations, the NNRP global analysis (Kalnay *et al.* 1996), and a simulation by the HadRM3 RCM. The NNRP reanalysis is model based, with a grid increment of about 210 km. The RCM has a grid increment of about 40 km, with LBCs provided by an AOGCM having about one-fourth the resolution. Clearly, the RCM produces rainfall extremes whose average magnitude is more consistent with the observations than that of the GCM-based NNRP reanalysis.

The following subsections will describe climate downscaling by classifying methods in different ways. First, the statistical and dynamical methods will be described and contrasted in Sections 16.3.1 and 16.3.2, respectively. Then, the use of both of these methods for downscaling future climates and current climates will be described in Sections 16.3.3 and 16.3.4, respectively. Lastly, a summary will be provided of how the downscaling methods have been applied to address different practical climate-dependent problems.

### 16.3.1 Statistical climate downscaling methods

#### Spatial statistical downscaling

Spatial statistical downscaling involves using linear or nonlinear statistical/empirical relationships to estimate small-scale local processes (the predictands, such as precipitation rate, temperature, or river discharge) based on features of the large-scale weather or



climate (the predictors) that are represented in (1) global reanalyses, (2) seasonal or annual predictions with AOGCMs, or (3) longer climate-forcing simulations with AOGCMs. Whether reanalyses or AOGCM output are used to define the predictors (for current-climate or future-climate downscaling), the general objective is to infer information about fine-scale processes without the use of a high-resolution model. A two-step process is involved. First, the statistical relationships are developed between the local climate variables of interest and the large-scale predictors, using local and large-scale data for the current climate. If observations of the local variables are not available for a geographic area, a LAM can be run for a range of large-scale regimes and a catalogue developed of local responses. In the second step, the statistical relationships are used to define the local system response to the large-scale features, for example in a future-climate simulated by an AOGCM. This statistical-downscaling process can be imagined as a parameterization of the local system response to the large-scale forcing, or as the establishment of analogs between the large- and small-scale features.

The choice of the predictor obviously depends on the predictand, given that a physical relationship must prevail. Two requirements exist for this choice: (1) it must be possible to diagnose the predictand accurately from the predictor and (2) the predictor must be well-predicted by the dynamic model or well-defined by the reanalysis. A third requirement, which may be more problematic, is that the predictor–predictand relationship must remain stationary during climate change. For diagnosis of precipitation on small scales, examples of predictors from the large-scale dynamic model are precipitation, sea-level pressure, relative humidity, geopotential height, wind direction, vorticity, and divergence (Wilby and Wigley 2000). The geographic area over which the predictor is defined should be sufficiently large to encompass the relevant large-scale processes. For example, Feddersen (2003) had to include a large fraction of the North Atlantic in order to represent the North Atlantic Oscillation (NAO) for the downscaling of seasonal precipitation predictions for Scandinavia.

Statistical relationships used in downscaling are typically calculated from observed or analyzed predictors and predictands. This is analogous to the perfect prognosis (perfect prog) approach to the statistical post processing of model weather forecasts, described in Chapter 13, where observations are used to define the algorithms that translate model output into information (e.g., variables) that cannot be obtained directly from the model. However, the large-scale dynamic models have biases, and thus the predictors produced by their forecasts will introduce errors in the downscaled variables. An alternative for defining predictor–predictand relationships for downscaling interseasonal predictions is to employ the approach used to generate MOS (Wilks 2006), also described in Chapter 13. Here, the predictands used to obtain the post-processing relationships are obtained from model forecasts, so the post processing of the model output corrects for the model's systematic errors. In the context of statistically downscaling climate forecasts, if the statistical downscaling relationship is based on model fields, the systematic errors in the model will automatically be accounted for. Unfortunately, as with the use of any MOS-based methods, a long series of historical climate reforecasts, or hindcasts, is needed in order to build the statistical relationships. And, these relationships must be regenerated any

time the model is upgraded because the systematic errors will change. Examples of the use of this method for defining the predictands in the statistical downscaling of seasonal predictions are found in Feddersen *et al.* (1999), Feddersen (2003), and Feddersen and Andersen (2005).

An obvious issue related to statistical climate downscaling is that it is limited by the assumption of temporal stationarity in the empirical relations. That is, an algorithm that is trained with current-climate data may not apply for future climates. Unfortunately, the nonstationarity in empirical climate relations is well documented (Ramage 1983, Slonosky *et al.* 2001, Charles *et al.* 2004). In contrast, Hewitson and Crane (2006) found that the nonstationarity can be relatively small. Of course the tuning to the current climate of parameters in physical-process parameterizations is of concern as well.

There are a number of different mathematical approaches for statistically relating the predictors on the large scale and the local variables, the predictands. Linear approaches are based upon regression models, while nonlinear approaches are based on weather-typing schemes and weather generators. See Zorita and von Storch (1999), Hanssen-Bauer *et al.* (2005), and Fowler *et al.* (2007) for further discussion of the different methods.

### Regression models

These methods directly quantify the relationship between the predictand and the predictor variables, and are classified as linear methods. A simple example described in Zorita and von Storch (1999) is based on the well-known correlation between the surface air temperature in Scandinavia and the NAO. In this case, a linear regression equation can be established between the anomaly in the NAO index (the sea-level pressure difference between the Azores and Iceland) and the anomaly in the temperature at a Scandinavian station. Thus, given changes in the NAO index in a future climate, the change in the Scandinavian temperature can be obtained from the regression equation. The technical complexity of the regression methods can be considerably greater than in this example, where the following mathematical constructs can be applied. See Zorita and von Storch (1999) and other references for discussion of the assumption, which is implicit in these methods, that the local variables are normally distributed.

- Simple/multiple regression (Hanssen-Bauer *et al.* 2003, Hay and Clark 2003, Johansson and Chen 2003, Matulla *et al.* 2003, Huth 2004, Hessami *et al.* 2008, Huth *et al.* 2008, Tolika *et al.* 2008),
- singular-value decomposition (Huth 1999, 2002; von Storch and Zwiers 1999; Widmann *et al.* 2003; Paul *et al.* 2008),
- canonical-correlation analysis (Wigley *et al.* 1990; von Storch *et al.* 1993; Busuioc *et al.* 2001, 2006, 2008; Chen and Chen 2003; Huth 2004; Xoplaky *et al.* 2004),
- empirical-orthogonal functions (Zorita and von Storch 1999, Benestad 2001, Wilby 2001), and
- principal-component analysis (Cubasch *et al.* 1996, Kidson and Thompson 1998, Hanssen-Bauer *et al.* 2003).

## Weather-typing schemes

Some of these approaches classify the large-scale weather in a region into a specific number of different, dominant weather regimes, patterns, or classes, based on a variable such as sea-level pressure or geopotential height. Then, the local weather (the predictand, say precipitation) is defined for each category based on the historical observation record. In contrast to the previous regression methods, where a grid-box value of a large-scale variable may be the predictor, here the pattern is the predictor. The downscaled climate, current or future, is defined by the frequency-of-occurrence of the predictor regimes. This method assumes that the same weather regimes will exist for future climates, and that the change will be represented by a new occurrence frequency for each of the regimes. The weather typing can be done through self-organizing maps, cluster analysis, or empirical-orthogonal functions. Alternatively, so-called analog or weather-classification schemes are based on a long record of observations of the large-scale weather and the local weather. The output from a GCM is compared to the large-scale observations for the period of record, the historical case where the observations best fit the GCM output is defined, and the simultaneously observed local weather is then associated with the case. Some examples of these methods follow:

- weather-classification/analog (Zorita and von Storch 1999, Palutikof *et al.* 2002, Díez *et al.* 2005, Timbal and Jones 2008), and
- self-organizing maps, cluster analysis, neural networks (Heimann 2001, Trigo and Palutikov 2001, Cavazos *et al.* 2002, Hewitson and Crane 2002, Gutiérrez *et al.* 2005, Moriondo and Bindi 2006, Huth *et al.* 2008, Tolika *et al.* 2008).

The downscaling relationships can be developed for large-scale data that pertain to different time scales. For example, monthly or seasonal anomalies on the global scales can be downscaled to produce corresponding anomalies on small scales. Or large-scale daily data can be downscaled. Buishand *et al.* (2004) discuss temporal aggregation levels for statistical downscaling of precipitation. For summaries of different statistical-downscaling methods, and their limitations and comparison, see Wilby *et al.* (1998), Haylock *et al.* (2006), and Busuioc *et al.* (2008).

## Temporal statistical downscaling

One of the motivations for the spatial downscaling of climate forecasts is to produce information on the scales that are needed for decision making. Similarly, it is important to provide data with sufficient temporal structure for these decisions. Time series of monthly or seasonal averages of future temperature or precipitation anomalies are useful for broad assessment of water-resources and agricultural impacts, but daily information is really needed for crop-yield models, and even finer time scales are needed, for example, for assessing the risk of flash floods. There are at least two issues. One is that statistical spatial downscaling may only provide monthly or seasonal anomalies. The other is that time series of variables that are associated with large AOGCM grid boxes are smoother than those that apply to single points, simply because of the averaging that is

implied over the large area. To address this need, synthetic high-resolution time series can be generated with what are called *stochastic weather generators*. For example, regarding precipitation, these generators can simulate the temporal distribution of wet and dry spells, the typical number of days with and without precipitation, and the intensity of precipitation. The generators can be tuned to apply to particular current and recent weather types. Information about the application of stochastic weather generators for climate-change studies can be found in Katz (1996), Semenov and Barrow (1997), Goddard *et al.* (2001), Huth *et al.* (2001), Palutikof *et al.* (2002), Busuioc and von Storch (2003), Katz *et al.* (2003), Wilby *et al.* (2003), Elshamy *et al.* (2006), Wilks (2006), and Kilsby *et al.* (2007).

### 16.3.2 Dynamical climate downscaling methods

Dynamical downscaling, or the dynamic-model-based generation of high-resolution climate conditions for a particular region and period of time, can be accomplished using a few different approaches (CCSP 2008). Each of the following methods can be used for current-climate or future-climate downscaling.

- Limited-area models (RCMs) are located over a geographical region of interest, and long simulations are produced by defining LBCs with output from an AOGCM or with a global analysis (Jones *et al.* 1995, 1997; Ji and Vernekar 1997; McGregor 1997; Gochis *et al.* 2002, 2003; Frei *et al.* 2003; Hay and Clark 2003; Roads *et al.* 2003a; Boo *et al.* 2004; Liang *et al.* 2004; Castro *et al.* 2005; Díez *et al.* 2005; Kang *et al.* 2005; Misra 2005; Paeth *et al.* 2005; Sotillo *et al.* 2005; Sun *et al.* 2005; Afiesimama *et al.* 2006; Antic *et al.* 2006; De Sales and Xue 2006; Druyan *et al.* 2006; Feser 2006; Liang *et al.* 2006; Moriondo and Bindi 2006; Woth *et al.* 2006; Christensen *et al.* 2007; Xue *et al.* 2007; Jiang *et al.* 2008; Lo *et al.* 2008; Rockel *et al.* 2008; Salathé *et al.* 2008).
- Global stretched-grid AGCMs (discussed in Chapter 3) use enhanced horizontal resolution over a geographic region of interest, and are run for climate time scales (Déqué and Piedelievre 1995, Lorant and Royer 2001, Gibelin and Déqué 2003, Déqué *et al.* 2005, Fox-Rabinovitz *et al.* 2006, Boé *et al.* 2007).
- Uniformly high-resolution AGCMs produce simulations of climate (Branković and Gregory 2001, May and Roeckner 2001, Duffy *et al.* 2003, Coppola and Giorgi 2005, Yoshimura and Kanamitsu 2008).
- Very-high-resolution orographic forcing is used in coarse-grid AOGCMs (Ghan *et al.* 2006, Ghan and Shippert 2006).

Instead of the typical grid increments of hundreds of kilometers for AOGCMs, models used for dynamical downscaling have grid increments of tens of kilometers or less. As with the use of high-resolution LAMs for weather prediction, the benefits of the resolution for climate prediction are attributable to (1) the better representation of fine-scale local forcing such as from orographic or other landscape variability, (2) the ability to explicitly represent processes rather than parameterize them, (3) the nonlinear interactions permitted

among a more-complete spectrum of waves, and (4) greater compatibility between the model's vertical and horizontal resolutions.

When the above approaches are used for future-climate downscaling, the downscaling models generally do not have ocean, ice, and vegetation dynamics, and thus the surface properties must be specified from (1) previously run parent, coarser-resolution AOGCM simulations or (2) global analyses for which ocean and surface conditions are specified. In common for all the approaches is the way that the downscaling models are run for time slices of a few decades, for example from 1961 to 1990 for a baseline climate and from 2070 to 2100 for a changed climate.

Even though global, multi-model ensemble climate-prediction methods have proven to be very valuable, opportunities for performing multi-model ensemble downscalings are limited by the fact that AOGCM output for many models is not archived with sufficient frequency to allow the use of the data to drive RCM LBCs. Another disadvantage of dynamic downscaling approaches is that the higher-resolution features represented in the atmosphere cannot interact with the ocean dynamics, and a departure of the large-scale atmospheric features in the downscaling model from those in the AOGCM means that the atmosphere–ocean interaction is negatively affected.

The following sections review the above-listed different approaches for dynamic downscaling.

### Limited-area models nested within AOGCMs or global analyses

An advantage of downscaling with RCMs is that the models are often very similar to mesoscale weather-prediction models that have already been developed and are well tested. The resolutions of the LAMs are simply adjusted so that they can be integrated for decades to centuries, with the computational resources available. Also, the use of RCMs for future-climate downscaling is appealing because the global-model output used for LBCs is easily accessed from the IPCC runs of past, present, and future climates that are archived at the Program for Climate Model Diagnosis and Intercomparison (PCMDI) at the Lawrence Livermore National Laboratory in the USA. And, for current-climate downscaling, high-quality global reanalyses are publicly available and easily accessible (Kalnay *et al.* 1996, Kanamitsu *et al.* 2002a, Upalla *et al.* 2005). Christensen *et al.* (2007) summarize a series of papers that describe results from the project entitled Prediction of Regional scenarios and Uncertainties for Defining European Climate change risks and Effects (PRUDENCE), a European study of dynamic downscaling that evaluated simulations of current and future climates using various RCMs. Also discussed were (1) the modeling of the specialized impacts of regional climate change on water resources, agriculture, ecosystems, energy, and transportation; (2) the modeling of extreme weather events; and (3) the policy implications associated with the availability of high-resolution climate predictions. Several other coordinated projects have applied RCMs for simulating regional climate change in various parts of the world: PIRCS for the USA (Takle *et al.* 1999), RMIP for Asia (Fu *et al.* 2005), ARCMIP for the Arctic (Curry and Lynch 2002, Rinke *et al.* 2005), and over the Pacific Ocean (Stowasser *et al.* 2007).

The impact of lateral boundaries on the solution of a LAM must be viewed somewhat differently in the context of climate downscaling. In Chapter 3 it was stated that, ideally, lateral boundaries should be sufficiently distant from the area of meteorological interest on a grid such that the negative effects of the boundaries do not contaminate the solution during the period of a forecast. However, for climate downscaling that involves running the LAM for years, this is not an option. In fact, there has been plentiful documentation of the strong sensitivity of downscaled climates to the exact position of lateral boundaries, the domain size of the RCM, and the quality of the data used for LBCs (Dickinson *et al.* 1989, Jones *et al.* 1995, Laprise *et al.* 2000, Denis *et al.* 2002, Rojas and Seth 2003, Seth and Rojas 2003, Dimitrijevic and Laprise 2005, Vannitsem and Chomé 2005, Diaconescu *et al.* 2007). In Section 10.4, a method was demonstrated for assessing the impact of the LBCs in RCM simulations. Denis *et al.* (2002) describe what are called Big-Brother–Little-Brother experiments, wherein a large domain RCM (Big-Brother) is used to establish a reference climate over an area, and short waves are filtered so that the RCM climate has scales similar to those of a GCM. This filtered reference climate is then used to provide LBCs for the same RCM (same resolution) that is run for a smaller domain (Little-Brother). The differences between the climate statistics from the Big- and Little-Brother integrations can then be attributed to LBC effects. Dimitrijevic and Laprise (2005), Antic *et al.* (2006), and Koltzow *et al.* (2008) use a similar method to evaluate LBC effects in downscaling with RCMs. Other applications of this method are referenced in Laprise *et al.* (2008) and Laprise (2008).

Because the RCM is intended to simulate the atmospheric response on small scales to the forcing by the global weather patterns, it is desirable if the regional model's large-scale solution does not depart significantly from that in the global data set. Unfortunately, if the models communicate only through the lateral boundaries of the regional model, the large-scale solution of the regional model can drift away from the imposed large scale (e.g., Jones *et al.* 1995). In order to reduce this problem for both future-climate and current-climate downscaling, a method is used called *spectral nudging* (Waldron *et al.* 1996; von Storch *et al.* 2000; Miguez-Macho *et al.* 2004; Castro *et al.* 2005; Kanamaru and Kanamitsu 2007a, 2008; Yoshimura and Kanamitsu 2008; Alexandru *et al.* 2009). Most applications of this method are based on the data-assimilation approach called Newtonian relaxation, or nudging, described in Chapter 6, wherein the model solution is nudged toward observations or gridded data using artificial terms in the prognostic equations. With spectral nudging, however, only the large-scale part of the regional-model solution is nudged toward the global data set, leaving the small scales unaffected.

For future- or present-climate downscaling, if sufficient computational resources exist the regional model can be run for many decades, with LBCs from AOGCMs or global reanalyses. However, to make the efforts more tractable, the downscaling may be done for selected time slices. For example, if a current-climate downscaling is required for a region, but only for, say, one season, the model can be run for time slices consisting of only the particular three months out of each year in the 40-year record of the NNRP reanalysis. For future-climate downscalings using output from AOGCM IPCC-scenario runs, the time-slicing can be more challenging because the existence of internal climate



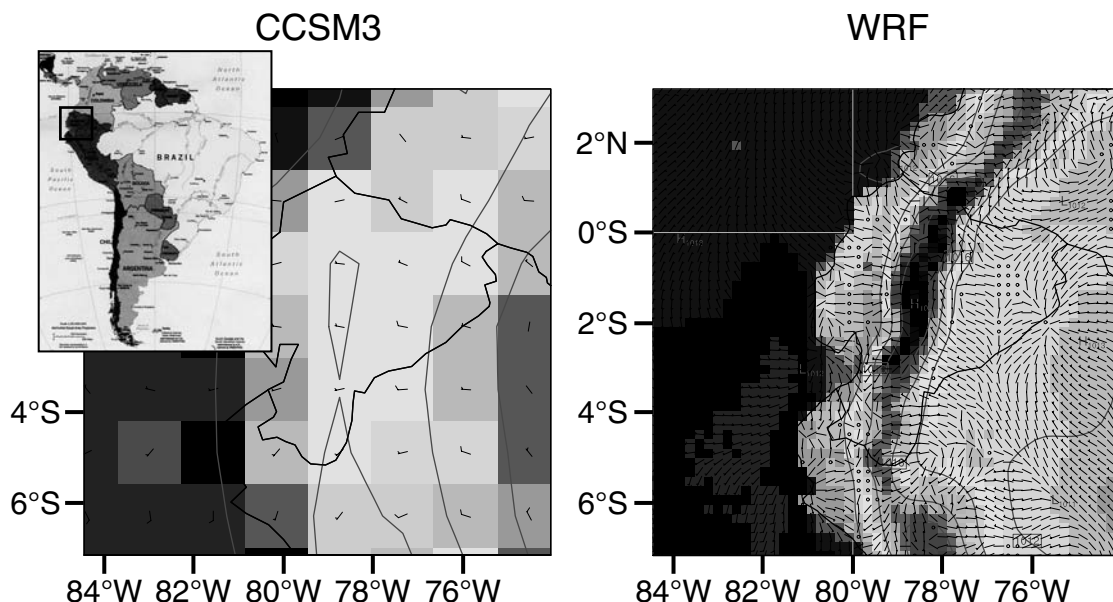


Fig. 16.11

Illustration of the difference in the horizontal resolution of simulations by the NCAR CCSM3 model with a grid increment of 250 km (left), and the WRF RCM with a grid increment of 10 km (right). The lateral-boundary conditions of WRF were forced by the CCSM simulation. Illustrated are the mean temperature and wind simulations from each model for the same period and geographic area. Darker grays represent lower temperature. The box in the map inset at the upper left shows the model study area over Peru. Provided by Andrew Monaghan, NCAR.

variability in the AOGCM output can cause the implied climate change in the region to depend on the time of the slices. For example, if an internal-variability cycle is at an extreme during the period of a slice, the downscaled climate during the time slice would not be representative of the more temporally averaged climate. This can be avoided by using long time slices, or by first evaluating the internal cycles in the AOGCM solution and avoiding the extremes. Another significant disadvantage of using short time slices is that the RCM does not have sufficient time to fully develop its own regional climate. Even though fine-scale responses to orography and coastlines will develop, recall that Pielke *et al.* (1999a) concluded that almost one year of simulation time may be required for a model to spin up its own soil moisture (for example, in response to fine-scale precipitation).

To illustrate the resolution benefits of downscaling with an RCM, Fig. 16.11 shows the mean temperature and winds over an area along the west coast of South America, for a period simulated by the NCAR Community Climate System Model 3 (CCSM3) AOGCM with a grid increment of 250 km, and the mean temperature and winds for the same region and period simulated by the WRF model with a grid increment of 10 km. The WRF RCM used the CCSM simulation for LBCs. In the CCSM mean temperatures, there is no evidence of the spine of the smoothed Andes Mountains, but the effect is clearly seen in the WRF solution.



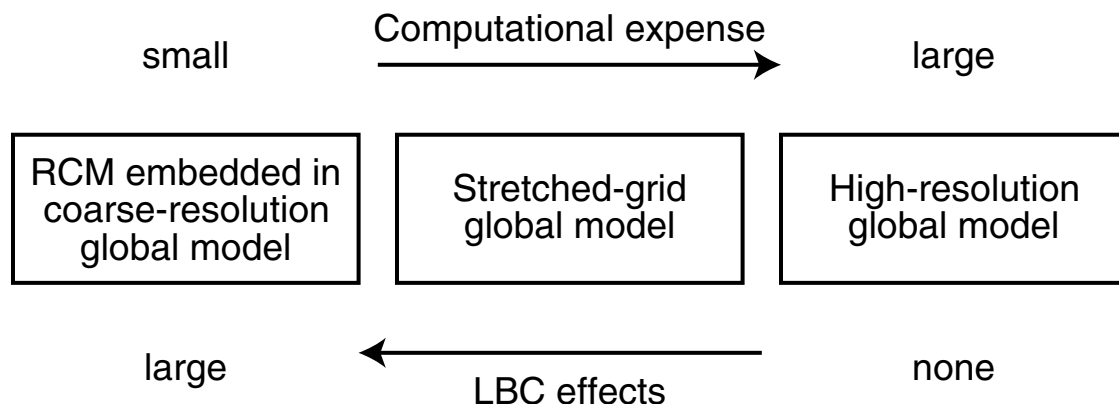
### Global variable-resolution (stretched-grid) AGCMs

These variable-resolution GCMs have enhanced, sometimes uniform, horizontal resolution over the geographic region for which a downscaled solution is needed (e.g., Déqué and Pielikevire 1995; Déqué *et al.* 1998; Fox-Rabinovitz *et al.* 2001, 2002, 2005, 2006; Gibelin and Déqué 2003). The fine grid is an integral part of the AGCM, with the transition in grid increment being gradual between the coarse-resolution and fine-resolution regions. Thus, unlike RCMs, there are no traditional LBC issues to deal with when using the stretched grids, and there is less potential error in the propagation of waves from the low-resolution to the high-resolution regions. Other claimed benefits of stretched-grid GCMs, relative to RCMs that are one-way nested within AOGCMs, include (1) the consistency in the parameterizations and the numerics between coarse and fine grids (thus ensuring greater spatial consistency in the model solution) and (2) the fact that processes represented on the regional grid can feed back to the global scales, which they cannot do with the one-way, parasitic nesting that is used with RCMs. Regarding point (1) above, it can, however, be argued that there are some situations where different parameterizations (e.g., convection) *should* be used in the regions with different horizontal resolution. Fox-Rabinovitz *et al.* (2006) describe a GCM Stretched-Grid Model Intercomparison Project (SGMIP).

These models have been run for times scales of seasons to decades in physical-process studies related to current regional climates. For example, Fox-Rabinovitz *et al.* (2001) use a stretched-grid GCM to study the anomalous regional climates associated with the 1988 US summer drought and the 1993 US summer flood. And Barstad *et al.* (2008) spectrally nudged a stretched-grid GCM to the ERA-40 analysis, where the resulting downscaled data set showed large improvements over the ERA-40 analysis. For example, the precipitation bias was reduced from 50% to 11%. For future-climate downscaling, Gibelin and Déqué (2003) obtain sea-surface temperature forecasts from a coarser-resolution coupled AOGCM, allowing their stretched-grid AGCM to simulate the future climate in the Mediterranean region for an IPCC scenario.

### Uniformly high-horizontal-resolution AGCMs

These AGCMs use relatively high horizontal resolution over the entire sphere in order to represent fine-scale processes, for time slices of AOGCM simulations. A disadvantage is obviously the high computational cost, which necessitates the use of time slices of modest length. Advantages include the lack of LBC problems that can be encountered with parasitically nested RCMs, and the uniformly high resolution means that small-scale processes in one region can interact with small-scale processes in another. Various studies have demonstrated the benefit of employing such higher horizontal resolution for climate simulations. Spectral nudging has been used to maintain the larger scales of the high-resolution simulation consistent with those of the coarser-resolution AOGCM simulations, while allowing fine-scale forcing from orography and other landscape features to develop regional climate features (von Storch *et al.* 2000, Yoshimura and Kanamitsu 2008). Figure 16.12 summarizes the relative strengths and weaknesses of the use of RCMs embedded within AOGCMs or global analyses, global variable-resolution

**Fig. 16.12**

Schematic comparing the LBC effects and computational costs of three approaches to high-resolution climate modeling. Adapted from original by Jack Katzfey, CSIRO.

(stretched-grid) AGCMs, and uniformly high-resolution AGCMs in terms of computational cost and LBC effects.

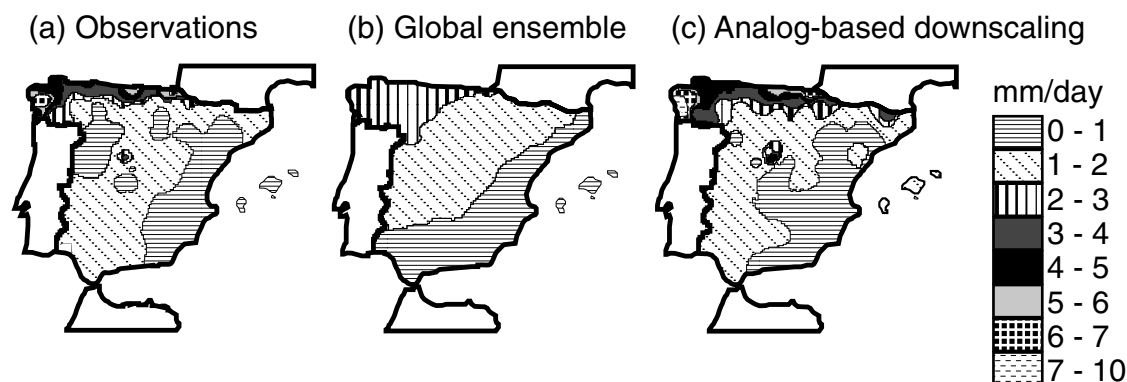
### Very-high-resolution orographic forcing in a coarse-grid AOGCM

This method uses a very-high-resolution surface-elevation data set to define the fractional area and mean elevation of a set of elevation classes, for each model grid cell. This information is then used during the simulation to define the vertical displacement of air flowing over the orography, where the effect of the Froude number is accounted for. The heating and moistening rates for each elevation class are area-weighted and applied to the grid-cell-mean conservation equations. Leung and Ghan (1995, 1998) developed and tested this method in a regional climate model, Ghan *et al.* (2002) applied it for a global-model downscaling simulation (with the NCAR CCSM) of western USA, and Ghan *et al.* (2006) tested it for a variety of other geographic regions worldwide.

### 16.3.3 Downscaling future climates

Future climate downscaling, using both dynamical and statistical methods, has been performed for every region of the world. As noted earlier, initial-value-based interseasonal and multi-year predictions can be downscaled, as can simulations of radiatively forced climate change. Many of the examples and citations in the previous two sections pertain to future-climate downscaling, and should be referenced for additional information.

Just as global models that are used for future-climate predictions are verified against observations of past or present climate, a similar process should be undertaken when downscaling with statistical or dynamical methods. That is, observations that define the present or past regional climates of an area should be used to verify the skill of the downscaling method. As noted earlier, for the verification of statistical methods the observations used in training the algorithm should not be used for verification. An example of the verification of a statistical downscaling process, using retrospective simulations of the current climate, is shown in Fig. 16.13. The observations define high average precipitation in northern Spain

**Fig. 16.13**

A comparison, for the current climate, of the regional precipitation for February through April in Spain, based on observations (a), the ensemble-mean of ECMWF and UK Met Office global-model simulations (b), and an analog-based statistical downscaling. Adapted from Palmer *et al.* (2004).

for February through April, with a maximum on the Atlantic coast (a). The analogous climate that is based on the ensemble-mean of ECMWF and UK Met Office global-model simulations (b) has no regional detail. An analog-based statistical downscaling reasonably reproduces the higher precipitation in the north, and the maximum to the west.

The following list provides examples of future-climate downscaling studies, for additional reading. Included are studies to define future regional climates, as well as evaluations of future-climate-downscaling methods using the current climate. One set of papers summarized by Iversen (2008) is related to the project Regional Climate Development under Global Warming (RegClim) that focusses on Northern Europe. See Fowler *et al.* (2007) for additional examples.

- *Asia* – Boo *et al.* (2004), Rupa Kumar *et al.* (2006), Chu *et al.* (2008), Ghosh and Mujumdar (2008), Paul *et al.* (2008), Zhu *et al.* (2008)
- *Europe* – Déqué and Piedelievre (1995), Jones *et al.* (1995, 1997), Zorita and von Storch (1999), Gibelin and Déqué (2003), Haylock *et al.* (2006), Boé *et al.* (2007), Bronstert *et al.* (2007), Ådlandsvik (2008), Beldring *et al.* (2008), Busuioc *et al.* (2008), Debernard and Røed (2008), Haugen and Iversen (2008), Hundechea and Bárdossy (2008), Huth *et al.* (2008), Tolika *et al.* (2008).
- *North America* – Wilby *et al.* (1998), Leung *et al.* (2004), Duffy *et al.* (2006), Liang *et al.* (2006), Gachon and Dibike (2007), Salathé *et al.* (2008)
- *South America* – Druyan *et al.* (2002)
- *Australia* – Timbal and Jones (2008)
- *Africa* – Lynn *et al.* (2005)

### 16.3.4 Downscaling current climates

To provide a historical context to current-climate downscaling, note that atmospheric models have been used for decades for filling space and time gaps among observations. For example, on global scales, long-term reanalyses have been generated with global-model

data-assimilation systems. The resulting MADS are used for analyzing trends, studying physical processes, and identifying erroneous observational data. On smaller scales, mesoscale models have been used in short simulations for case study analyses, using LBCs from global MADS, where good model-simulation skill at observation locations has been justification for believing the simulation in the space and time gaps between the observations. In both cases, the strength of using the models to fill the observation gaps is that the fields are dynamically consistent and they are defined on a regular grid. Additionally, the models respond to local forcing that adds information beyond what can be represented by the observations. More recently, the availability of greater computing power has allowed the generation of long-term mesoscale analyses using downscaling methods, where the resulting gridded data sets are used for various applications. For example, mesoscale analyses can be used to define the statistical distribution of wind speeds for wind-energy “prospecting”. Boundary-layer climatologies can be used with transport and diffusion or air-quality models to define prevailing patterns in source–receptor relationships. Also, such boundary-layer climatologies can allow an assessment of the statistical risk to populations of the release of hazardous material into the atmosphere from chemical or nuclear-power-generation facilities. Lastly, the automated interpretation of long-period reconstructions of the atmosphere can be used to define physical processes in ways that are much more robust than obtainable from the use of a few case studies.

Mesoscale reanalyses are used to fill both small and large space and time gaps. In regions with plentiful radiosonde data, the spatial voids may be only a few hundred kilometers in size. In other areas of the world, there are large expanses without data, either because there are no observations or because data have not been archived. Of course the oceans of the world represent large voids where models and satellite data must be relied upon for estimates of atmospheric properties and processes.

For future-climate downscaling, discussed in the last section, the RCM’s solution is determined by the LBCs and the surface forcing. But, for current-climate downscaling, observations are available to help define the model’s solution for the regional climate. The model can be restarted periodically, in an intermittent-assimilation process, or observations can be assimilated continuously through Newtonian relaxation or other methods. For example Hahmann *et al.* (2010) describe the use of Newtonian relaxation (Stauffer and Seaman 1994) in a WRF-based RCM used for current-climate downscaling. And Nunes and Roads (2007a,b) showed the benefits of precipitation assimilation in regional downscaling. When RCMs are restarted at regular intervals from new initial conditions, for example to assimilate observations or to maintain consistency with the large-scale analysis, the model may never fully spin up its own internal regional climate. Even though the RCM solution will contain small-scale thermally or orographically forced features, which is obviously value added to what is available from the coarse analysis, the restarts can prevent the model from developing its own soil moisture equilibrium and land–atmosphere feedbacks.

In order for a MADS to be used for a particular purpose, the veracity of the analysis needs to be verified in the context of the application. For example, for wind-energy-prospecting purposes, the model must be able to reasonably reproduce the PDF of the wind speed at the height of the generator. Because the generation equipment is vulnerable

to speeds above a threshold, it would be especially important that the model capture the upper tail of the speed PDF. Similarly, for air-quality or other transport and diffusion modeling applications, the boundary-layer depth and static stability must be simulated accurately, as must the mean wind in the boundary layer.

Specific applications of a MADS also dictate how the data must be interpreted. That is, translating a reanalysis data set into useful and intuitively understandable climatological information generally goes beyond the calculation of simple, conventional climate statistics. Further processing may be necessary to classify the data into different weather regimes as a function of time of day and season. It may be necessary to define a “typical day” in July over a particular area, in terms of the wind field, or the precipitation distribution, and this product is clearly not the climatological mean. And, for many applications, the complete PDF of a variable is needed; for example, for hydrologic purposes the PDF of rainfall intensity is essential.

An example of the use of an RCM (MM5) for current-climate downscaling is shown in Fig. 16.14. In this case, the ability of the model to replicate the climate of 60-m AGL

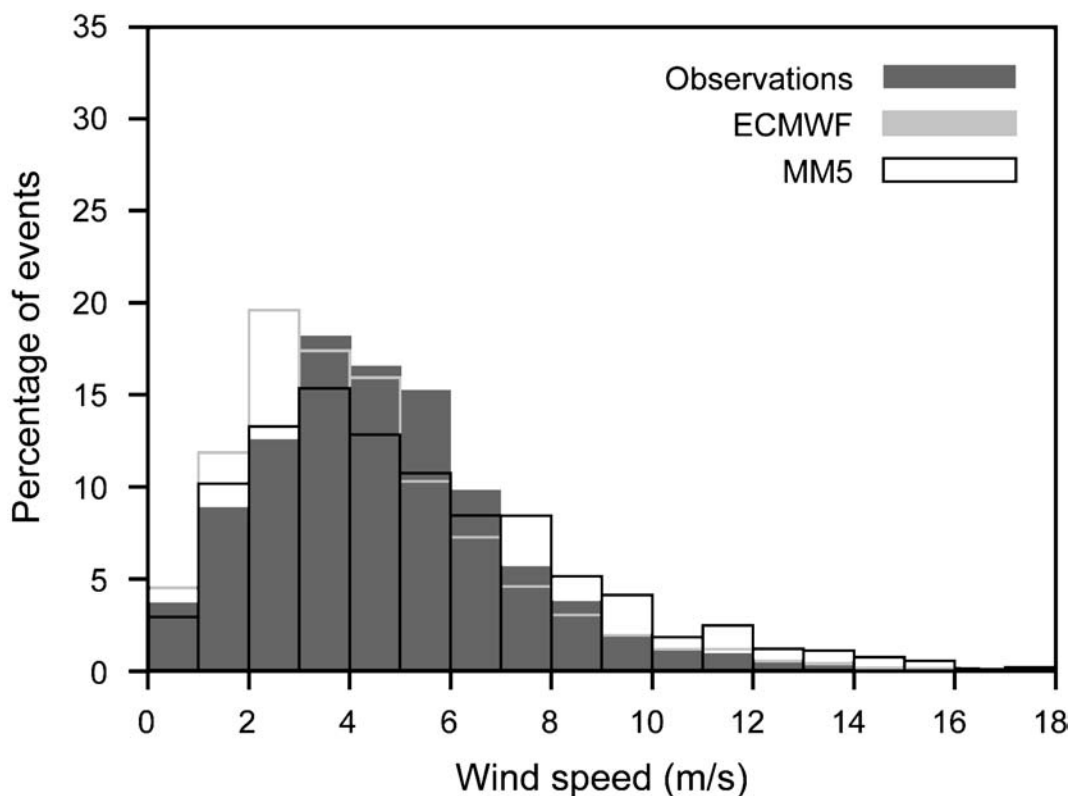


**Fig. 16.14** Frequency distribution of 60-m AGL wind speed at a location on the Eastern Mediterranean coast, based on observations (dark gray), a downscaling simulation by the MM5 RCM (black line), and the ECMWF global model (light gray line) for 10 Januaries from 1998 to 2007. Adapted from Hahmann *et al.* (2010).

winds has implications for wind-power generation. The figure depicts the frequency distribution of observed wind speed at a location on the eastern coast of the Mediterranean, for the month of January during the period 1998–2007. Also shown are the frequency distributions based on the ECMWF analysis, and the MM5 model that was used to downscale from the NNRP analysis. This clearly shows that added model resolution does not always produce improved PDFs. The RCM better defines the low-speed part of the spectrum, but the global reanalysis is better at the higher speeds.

Another example of a current-climate dynamic downscaling by an RCM (WRF model) is shown in Fig. 16.15. Here, the WRF model's LBCs are forced by the North American Regional Reanalysis (NARR, Mesinger *et al.* 2006) in a six-month simulation for a region of the Rocky Mountains in western Colorado that is the source of the water for the Colorado River. The WRF grid increment was 2 km and the NARR's is 32 km. Shown in the figure is the cumulative precipitation (liquid equivalent) for the period of the winter- and spring-season simulation, averaged over 120 snow observation locations (SNOW TELemetry - SNOTEL), based on the NARR and the WRF RCM simulation. The NARR and WRF precipitation values were bilinearly interpolated to the SNOTEL locations. In this case, the RCM clearly added value to the coarser reanalysis. The expectation is that such a downscaling with an RCM could be similarly beneficial for downscaling future climates.

Some dynamic downscalings of the current climate have been performed to provide gridded publicly available data sets for community use, in the same way that the NNRP,

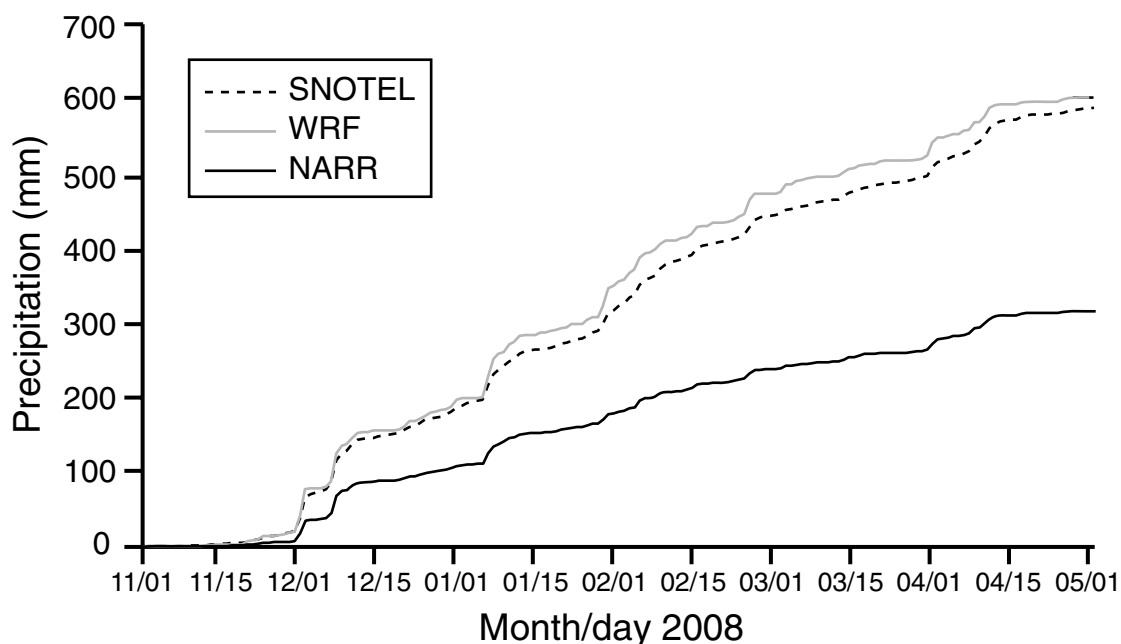


Fig. 16.15

Cumulative liquid-equivalent precipitation over the headwaters of the Colorado River in Western Colorado, for six winter and spring months, based on observations (120 SNOTEL sites), the NARR, and the WRF RCM (2-km grid increment). Observed and analyzed values are averages for the 120 locations. Provided by Roy Rasmussen, NCAR.

NCEP-DOE, MERRA, and ERA-40 analyses have been generated on the global scale. For example, the NARR has been created for North America and adjacent ocean areas using NCEP's Eta-model (Janjić 1994) Data-Assimilation System (EDAS). Unlike the global analysis systems, the EDAS that was used to construct the NARR assimilated high-quality precipitation observations. Thus, the land-surface state is more-accurately defined, as is the land-atmosphere interaction. This makes the analysis more valuable for hydrologic studies. The horizontal grid increment of the NARR is 32 km, there are 45 levels in the vertical, and LBCs are provided by the NCEP-DOE (R-2) global reanalysis. The reanalysis spans the 25-year period from 1979 to 2003, but its production has been continued beyond 2003 in near-real time using a Regional Climate Data Assimilation System. Another long-period current-climate downscaling for North America was performed for the period 1950–2002 using the RAMS model (Castro *et al.* 2007a,b). For the area of California, a 57-year regional reanalysis has been produced, with a 10-km grid increment, for applications in various climate studies (Kanamitsu and Kanamaru 2007, Kanamaru and Kanamitsu 2007b). Publicly available regional reanalyses are also being prepared for other areas, such as Europe and the Arctic.

The following list provides example references to additional efforts that used current-climate downscaling methods to study the regional climate of an area, or the prevailing physical processes.

- *Asia* – Ji and Vernekar (1997), Fox-Rabinovitz *et al.* (2002), Kang *et al.* (2005)
- *Europe* – Heimann (2001), Frei *et al.* (2003), Fil and Dubus (2005), Sotillo *et al.* (2005), Žagar *et al.* (2006), Boé *et al.* (2007)
- *North America* – Stensrud *et al.* (1995), Fox-Rabinovitz *et al.* (2001, 2002, 2005), Gochis *et al.* (2002, 2003), Hay and Clark (2003), Widmann *et al.* (2003), Liang *et al.* (2004), Duffy *et al.* (2006), Xue *et al.* (2007)
- *South America* – Fox-Rabinovitz *et al.* (2002), Roads *et al.* (2003b), Rojas and Seth (2003), Seth and Rojas (2003), Misra (2005), Sun *et al.* (2005), Rauscher *et al.* (2007)
- *Australia* – Fox-Rabinovitz *et al.* (2002), Mehrotra *et al.* (2004)
- *Africa* – Fox-Rabinovitz *et al.* (2002), Song *et al.* (2004), Paeth *et al.* (2005), Afiesimama *et al.* (2006), Druryan *et al.* (2006, 2007), Anyah and Semazzi (2007)

### 16.3.5 Examples of practical problems addressed by climate downscaling

It was noted earlier that climate impacts must typically be forecast, understood, and dealt with at the local and regional levels. This need has motivated many of the current-climate and future-climate downscaling activities. Some examples of the practical problems that have been addressed by the hundreds of downscaling studies are provided in Table 16.5. This table does not include the many other downscaling studies that have been used for (1) the evaluation and comparison of downscaling methods, (2) long-term mesoscale physical-process studies, and (3) the verification of downscaling schemes for the present climate, so that they may be used with greater confidence in downscalings of future climates. Fowler and Wilby (2007) introduce a series of papers that describe downscaling techniques employed in hydrological impact studies.



**Table 16.5** Examples of the practical problems that have been addressed by downscaling studies. Listed are (1) the application of the study; (2) whether the downscaling was dynamically (D) or statistically (S) based; (3) if the downscaling was applied to future-climate simulations (not current), was the simulation for forced climate change (GG, greenhouse gas) or based on initial conditions (IC); (4) the relevant geographic area; and (5) references.

Application	Dynamical or statistical	GG-forced or IC global forecast, or current	Geographic area	References
Water resources, drought, flood	S	IC	UK	Wilby <i>et al.</i> 2004, 2006
	S and D	GG	UK	Haylock <i>et al.</i> 2006, Bell <i>et al.</i> 2007
	D	GG	Europe	Hanson <i>et al.</i> 2007, Blenkinsop and Fowler 2007
	S and D	GG	Germany	Bronstert <i>et al.</i> 2007
	S	GG	Australia	Charles <i>et al.</i> 2007, Timbal and Jones 2008
	S and D	IC	Spain	Diez <i>et al.</i> 2005
	S	GG	Greece	Tolika <i>et al.</i> 2008
	D	current	North America	Brochu and Laprise 2007
	D	GG	North America	Salathé Jr. <i>et al.</i> 2007, 2008
	S	GG	East Asia	Paul <i>et al.</i> 2008
Air quality	D	GG	Houston, USA	Jiang <i>et al.</i> 2008
Wind energy	S and D	GG	Europe	Pryor <i>et al.</i> 2005a, b; 2006
	S	current	Europe	Heimann 2001, Landberg <i>et al.</i> 2003
Wave, storm surge	D	GG	North Sea	Woth <i>et al.</i> 2006, Debernard and Røed 2008
General weather	D	GG	USA	Liang <i>et al.</i> 2006, Salathé Jr. <i>et al.</i> 2008, Leung <i>et al.</i> 2004, Duffy <i>et al.</i> 2006
Crop development, agriculture	S and D	GG	Italy	Moriondo and Bindi 2006, Marletto <i>et al.</i> 2005
Radioactive waste disposal	D	current	USA	Dickinson <i>et al.</i> 1989
Forestry	D	GG	Europe	Hanson <i>et al.</i> 2007
Energy use	D	GG	Europe	Hanson <i>et al.</i> 2007
Tourism	D	GG	Mediterranean	Hanson <i>et al.</i> 2007
Insurance	D	GG	Europe	Hanson <i>et al.</i> 2007
Temperature extremes	D	current	Canada	Gachon and Dibike 2007
	S	IC	Spain	Frías <i>et al.</i> 2005
Hurricanes	D	GG	Atlantic	Knutson <i>et al.</i> 2008

## 16.4 Modeling the climate impacts of anthropogenic landscape changes

Atmospheric models are good tools for evaluating the impact of historical or future landscape changes on climate. Specifically, a simulation is performed with the landscape that prevailed before the change, a second simulation is performed based on the landscape that prevailed after the change, and the differences in the associated weather and climate are documented. Sometimes, short simulations focus on weather impacts, from which can be inferred climate impacts. Or, such pairs of simulations can be conducted for longer periods to allow more-direct calculation of climate statistics. If the experiments are performed for historical periods, the motivation is generally to develop a better understanding of land–atmosphere interactions that could have led to regional-climate change in the recent past. Alternatively, estimates of possible future changes in the landscape can be used in “what if” experiments – that is, what will be the impact on the regional climate if specific anthropogenic changes occur, such as continued urbanization, conversion of an area of grassland to farming, changing irrigation practices, or desertification. These studies are generally conducted using GCM, or coupled GCM-RCM, simulations of the present large-scale climate, but sometimes climate-forcing effects are included along with prescribed, expected anthropogenic landscape changes.

Even though there clearly are local-climate effects of landscape change, it is estimated that humans have modified one-third to one-half of the land surface area of Earth, and the aggregate effect of this could influence global-scale circulations as well. For example, Pielke (2005) states that landscape effects may be just as important in altering the weather as changes in climate patterns associated with greenhouse gases, and he further points out that anthropogenic landscape changes are not adequately accounted for in IPCC simulations.

### 16.4.1 Modeling the effects on local and regional climate of specific anthropogenic landscape changes

The following sections describe a few of the different types of anthropogenic landscape change for which the climate impacts have been modeled.

#### Urbanization and suburbanization

Even though urban regions cover only about 0.2% of Earth’s land surface, their impacts on local and regional climate can be substantial. Thus, urban landscapes must be accurately mapped (Jin and Shepherd 2005), and their physical properties must be included in the land-surface components of RCMs. The urban heat island is a well-known impact of urbanization on local climate, where the thermal effect can be 5–10 °C. An example of a study that looked at both the anthropogenic landscape changes associated with future urbanization as well as greenhouse forcing is Jiang *et al.* (2008). For the city of Houston

(USA), the coupled CCSM and WRF-Chem models were run for a current time slice and for a future time slice (2051–2053) for the A1B emissions scenario. The WRF RCM's land surface for the future-climate simulation was defined based on the landscape changes expected from the growth of the city. The WRF-Chem model was used because the objective was to predict the impacts on surface ozone concentrations. Other examples are Pielke *et al.* (1999b) and Marshall *et al.* (2004) who use multi-month RCM simulations to show the significant impact on regional climate of the development of the Florida Peninsula during the last century.

### Deforestation and the expansion of agriculture

The area involved in this type of landscape change is immense, and numerous modeling studies have evaluated its impacts on regional climate. For example, Strack *et al.* (2008) used an RCM and a landcover data set for the eastern USA to estimate the regional climate for the years 1650, 1850, 1920, and 1992, which span the deforestation and expansion of agriculture that has occurred since European settlement began. Since 1650, the model simulations showed an increase in maximum and minimum daily temperatures by 0.3–0.4°C, with most of the change occurring before 1920. Adegoke *et al.* (2006) found similar important climate effects of landscape change in the US High Plains. For example, cloud development occurred almost two hours earlier over agricultural land than over forested areas. Even though it might be imagined that desert climates would remain unaffected by anthropogenic impacts, Beltrán-Przekurat *et al.* (2008) demonstrated that the conversion of grassland to shrubland in the Chihuahuan Desert, through overgrazing in the last 150 years, had significant impacts on the regional climate. And, in a study of tropical landscape modification, Lawton *et al.* (2001) showed the impact of deforestation in Costa Rica on ecosystems in adjacent mountains. And for Africa, Semazzi and Song (2001) evaluated the potential effect on climate of the deforestation of the tropical rain forests.

### Agricultural irrigation

As agriculture has expanded into semi-arid lands, large areas have become irrigated so that their soil moisture far exceeds natural values. Models have shown a significant impact on regional climate. Segal *et al.* (1989) employed a LAM and observations to study the atmospheric effects of irrigation in eastern Colorado (USA), and demonstrated a significant impact. Yeh *et al.* (1984) used a simple global model to show that large-scale irrigation has an effect on regional climate, and especially precipitation. Chang and Wetzel (1991) employed a LAM to show that spatial variations in soil moisture and vegetation affect the evolution of the prestorm convective environment in the eastern Great Plains of North America. Beljaars *et al.* (1996) documented that model precipitation forecasts of extreme rainfall events in July 1993 in the Midwest USA were strongly related to soil-moisture anomalies about one day upstream. Paegle *et al.* (1996) related model-simulated rainfall for the same period to local evaporation, where the link was through effects on the low-level jet. Chen and Avissar (1994) demonstrated that landscape discontinuities (such as those associated with boundaries between irrigated and nonirrigated land) enhance

shallow convective precipitation. Chase *et al.* (1999) and Chen *et al.* (2001) show how conversion of semi-arid grasslands to dry farmland and irrigated farmland in northeastern Colorado affected the local atmospheric conditions as well as the rainfall in the mountains to the west.

### 16.4.2 Modeling the effects on global climate of anthropogenic landscape change

Because of the large land-surface area that has been modified by humans, it is reasonable that the aggregate effect could be sufficiently large to influence global-scale weather patterns and climate. Feddema *et al.* (2005) describe experiments with an AOGCM that were designed to evaluate this large-scale impact. By adding the effects of global land cover changes in simulations of IPCC scenarios A2 and B1, they showed the influence of landscape-change impacts on many aspects of regional climate, as well as effects on the global circulation. For example, in simulations to 2100 for the A2 scenario, agricultural expansion over the Amazon influenced the Hadley circulation, monsoon circulations, and the location of the ITCZ, which in turn affected extratropical climates. Also, in simulations with an AGCM, Chase *et al.* (2000) showed that tropical landscape changes altered the high-latitude Northern Hemisphere winter climate, including pushing the westerly jet farther north. Pielke (2002b) claims that anthropogenic landscape change has been overlooked in the IPCC assessments.

### SUGGESTED GENERAL REFERENCES FOR FURTHER READING

#### AOGCM simulations

- AchutaRao, K., C. Covey, C. Doutriaux, *et al.* (2004). *An Appraisal of Coupled Climate Model Simulations*. Lawrence Livermore National Laboratory report UCRL-TR-202550, 16 August 2004.
- Giorgi, F. (2005). Climate change prediction. *Climate Change*, **73**, 239–265, doi: 10.1007/s10584-005-6857-4.
- Hurrell, J., G. A. Meehl, D. Bader, *et al.* (2009). A unified modeling approach to climate system prediction. *Bull. Amer. Meteor. Soc.*, **90**, 1819–1832.
- IPCC, 2007: *Climate Change 2007: The Physical Science Basis. Contribution of Working Group I to the Fourth Assessment Report of the Intergovernmental Panel on Climate Change*, S. Solomon, D. Qin, M. Manning, *et al.* (eds.). Cambridge, UK: Cambridge University Press.
- McGuffie, K. and A. Henderson-Sellers (2001). Forty years of numerical climate modeling. *Int. J. Climatol.*, **21**, 1067–1109.

#### Seasonal to interannual simulations

- Goddard, L., S. J. Mason, S. E. Zebiak, *et al.* (2001). Current approaches to seasonal-to-interannual climate predictions. *Int. J. Climatol.*, **21**, 1111–1152.
- Shukla, J., J. Anderson, D. Baumhefner, *et al.* (2000). Dynamical seasonal prediction. *Bull. Amer. Meteor. Soc.*, **81**, 2593–2606.

## Climate downscaling

- Feser, F. (2006). Enhanced detectability of added value in limited-area model results separated into different spatial scales. *Mon. Wea. Rev.*, **134**, 2180–2190.
- Fowler, H. J., S. Blenkinsop, and C. Tebaldi (2007). Linking climate change modelling to impacts studies: Recent advances in downscaling techniques for hydrological modelling. *Int. J. Climatol.*, **27**, 1547–1568.
- Hanssen-Bauer, I., E. J. Førland, J. E. Haugen, and O. E. Tveito (2003). Temperature and precipitation scenarios for Norway: comparison of results from dynamical and empirical downscaling. *Climate Res.*, **25**, 15–27.
- Hewitson, B. C., and R. G. Crane (1996). Climate downscaling: Techniques and application. *Climate Res.*, **7**, 85–95.
- Laprise, R. (2008). Regional climate modelling. *J. Comput. Phys.*, **227**, 3641–3666.
- Laprise, R., R. de Elía, D. Caya, *et al.* (2008). Challenging some tenets of regional climate modeling. *Meteorol. Atmos. Phys.*, **100**, 3–22.
- Wilby, R. L., and T. M. L. Wigley (1997). Downscaling general circulation model output: a review of methods and limitations. *Prog. Phys. Geog.*, **21**, 530–548.

## Modeling the impacts of anthropogenic landscape changes on climate

- Feddema, J. J., K. W. Oleson, G. B. Bonan, *et al.* (2005). The importance of land-cover change in simulating future climates. *Science*, **310**, 1674–1678.
- Pielke, R., Sr. (2005). Land use and climate change. *Science*, **310**, 1625–1626.
- Pielke, R. A., Sr., J. Adegoke, A. Beltrán-Przekurat, *et al.* (2007). An overview of regional land-use and land-cover impacts on rainfall. *Tellus*, **59B**, 587–601.
- Pielke, R. A., G. Marland, R. A. Betts, *et al.* (2002). The influence of land-use change and landscape dynamics on the climate system: relevance to climate-change policy beyond the radiative effect of greenhouse gases. *Phil. Trans. R. Soc. Lond.*, **360**, 1705–1719.

## PROBLEMS AND EXERCISES

1. Learn how to access the IPCC-model output at a website provided by your instructor, and use the data to briefly illustrate climate change for a particular geographic area.
2. In interpreting output from current- or future-climate downscalings, it is common to want to define a “typical day” rather than simply looking at mean values or PDFs of variables. Explain possible approaches for doing this.
3. Summarize the types of land–atmosphere–biosphere feedbacks that should be represented in models that are used for studies of the impacts on regional climate of anthropogenic landscape changes.
4. Explain specific examples of the component-level testing of climate models.
5. Summarize the types and time scales of the different cycles that contribute to the internal variability of the climate system.
6. Based on your knowledge of physical processes, suggest some reasonable choices for predictors, for different predictand variables.

7. Describe the types of applications of climate models for which PDFs of model variables would be especially important.
8. Internal variability in the climate system, on time scales of years to decades, is relevant to the problem of modeling radiatively forced climate change. Is there variability on shorter time scales that must be understood and accounted for when interpreting seasonal climate predictions?
9. How can Rossby phase-speed errors associated with a particular dynamical core have consequences for climate prediction?